THESIS FOR THE DEGREE OF DOCTOR OF PHILOSOPHY

Aging-Aware Classification and Optimal Usage of Electric Vehicle Batteries

Huang Zhang

Department of Electrical Engineering
Chalmers University of Technology
Gothenburg, Sweden, 2025

Aging-Aware Classification and Optimal Usage of Electric Vehicle Batteries

Huang Zhang
ISBN 978-91-8103-200-0

Acknowledgements, dedications, and similar personal statements in this thesis, reflect the author's own views.

Selected material from the author's licentiate thesis: Huang Zhang, "Interpretable Battery Lifetime Prediction Using Early Degradation Data", *Chalmers University of Technology*, Gothenburg, Sweden, May 2023, is republished in this Ph.D. thesis.

Doktorsavhandlingar vid Chalmers tekniska högskola
Ny serie nr 5658
ISSN 0346-718X

Department of Electrical Engineering
Chalmers University of Technology
SE-412 96 Gothenburg, Sweden
Phone: +46 (0)31 772 1000

Cover:
An illustration of battery lifecycle management from cradle to grave.

Printed by Chalmers Digital Printing
Gothenburg, Sweden, May 2025

Aging-Aware Classification and Optimal Usage of Electric Vehicle Batteries

Huang Zhang
Department of Electrical Engineering
Chalmers University of Technology

Abstract

To facilitate successful market adoption of second-life battery energy storage systems (BESSs) based on new and used electric vehicle (EV) batteries, we propose aging-aware classification in first-life applications and optimal usage in second-life applications of EV batteries.

Specifically, a transferable physics-informed framework is proposed for battery degradation mode estimation and phase detection, and a quantile regression forests (QRF) model is proposed for battery lifetime early prediction, which enables aging-aware classification of EV batteries. For optimal usage of EV batteries in second-life BESS applications, an economic stage cost function is proposed to account for both the grid and the battery degradation cost, and an automatic kernel search method is extended to construct the best composite kernel for Gaussian process (GP) regression models in two battery applications. The fine-tuning strategy is proven to be effective in improving online battery degradation mode estimation and phase detection performance in the target first-life application. The QRF model can provide cycle life point prediction with high accuracy, and uncertainty quantification as the width of prediction intervals. The implicit policy incorporating historical operational data and "fixed" forecasted electricity price achieves the best economic performance, and GP regression models with the best kernel can provide better prediction performance in the two battery applications.

In summary, machine learning methods are proposed in this thesis to enable aging-aware classification in first-life applications and optimal usage in second-life applications of EV batteries, which hopefully facilitates the market adoption of second-life BESSs based on new and used EV batteries.

Keywords: Lithium-ion batteries, battery lifetime prediction, battery degradation diagnosis, energy management, interpretable physics-informed machine learning.

To cross the swamp, not to chase all the butterflies or fight all the alligators.

List of Publications

This thesis is based on the following publications:

[A] **Huang Zhang**, Yang Su, Faisal Altaf, Torsten Wik, and Sébastien Gros, "Interpretable Battery Cycle Life Range Prediction Using Early Cell Degradation Data". *Published in IEEE Transactions on Transportation Electrification, Dec. 2022.*

[B] **Huang Zhang**, Faisal Altaf, Torsten Wik, and Sébastien Gros, "Comparative Analysis of Battery Cycle Life Early Prediction Using Machine Learning Pipeline". *Published in proceedings of the 22nd IFAC World Congress, Yokohama, Japan, Jul. 2023.*

[C] **Huang Zhang**, Faisal Altaf, and Torsten Wik, "Scenario-Aware Machine Learning Pipeline for Battery Lifetime Prediction". *Published in proceedings of 2024 European Control Conference, Stockholm, Sweden, Jul. 2024.*

[D] **Huang Zhang**, Faisal Altaf, and Torsten Wik, "Battery Capacity Knee-Onset Identification and Early Prediction Using Degradation Curvature". *Published in Journal of Power Sources, Jul. 2024.*

[E] **Huang Zhang**, Xixi Liu, Faisal Altaf, and Torsten Wik, "A Transferable Physics-Informed Framework for Battery Degradation Diagnosis, Knee-Onset Detection and Knee Prediction". *Submitted.*

[F] **Huang Zhang**, Faisal Altaf, and Torsten Wik, "Comparative Study of Aging-Aware Control Strategies for Grid-Connected Photovoltaic Battery Systems". *Published in proceedings of the 63rd IEEE Conference on Decision and Control, Dec. 2024.*

[G] **Huang Zhang**, Xixi Liu, Faisal Altaf, and Torsten Wik, "A Practitioner's Guide to Automatic Kernel Search for Gaussian Processes in Battery Applications". *Submitted to the 64th IEEE Conference on Decision and Control, Dec. 2025.*

Other publications by the author, not included in this thesis, are:

[H] **Huang Zhang**, Faisal Altaf, and Torsten Wik, "Synthetic Dataset of LG M50 Batteries with Different Degradation Pathways". *Published in Data in Brief*, Dec. 2024.

[I] **Huang Zhang**, and Torsten Wik, "Spectral Analysis of Approximated Capacity Fade Curvature for Lithium-Ion Batteries". *Accepted for the 38th International Electric Vehicle Symposium and Exhibition*, Gothenburg, Sweden, Jun. 2025.

[J] Yang Su, **Huang Zhang**, Benoit Gabrielle, and David Makowski, "Performances of Machine Learning Algorithms in Predicting the Productivity of Conservation Agriculture at a Global Scale". *Published in Frontiers in Environmental Science*, Feb. 2022.

Acknowledgments

Multiple times during my doctoral studies, I was mentally and emotionally drained and asked why I was here. Then I usually took a walk in the little forest near my office. During the walk, I recalled that I was here simply because I wanted to satisfy my curiosity by sailing and sometimes diving into the ocean of knowledge. I chose this journey with sufficient autonomy at the beginning! However, this journey has never been easy, but I knew I was not alone, especially in the dark Swedish winter.

First, I want to thank my supervisors, Prof. Torsten Wik and Dr. Faisal Altaf, for their invaluable support and encouragement toward an independent researcher. I am grateful to both of you for allowing me a great degree of autonomy in finding my research niche. I truly enjoyed our research and non-research discussions during my doctoral studies. In addition, I would like to thank Prof. Sébastien Gros for his supervision from the beginning until my licentiate. I also want to express my gratitude to my examiner, Prof. Nikolce Murgovski, who was willing to step in after my licentiate seminar. A very special thank you goes to my discussion leader Dr. Eibar Flores from the SINTEF Industry who gave constructive feedback on my research progress at my licentiate seminar.

I must express my sincere appreciation to Volvo Group and Swedish Energy Agency for funding my doctoral studies through grant No. 45540-1 and P2024-00998. In particular, I am deeply grateful for the support from my manager Olle Friberg, and former managers Björn Fridholm, Naima Abdikader, and Karl Palmlin at Volvo Group Trucks Technology. I also thank Ylva Olofsson from Volvo Energy and Pierre Hult from Riksbyggen for providing the information about a grid-connected microgrid studied in this thesis. Ian Mathews from Sensai Analytics, I learned a lot about techno-economic modeling of batteries from our meetings. I wish you and your business all the best! My gratitude is also extended to Anton Klintberg and Faouzi Al Mouatamid for their encouragement at the beginning of my doctoral studies, and Carlos de Mattos for satisfying my curiosity about Brazilian culture.

I want to thank fellow PhD students with whom I started my journey. In particular, Angel Molina Acosta, Sten Elling Tingstad Jacobsen, Anand Ganesan, and Konstantinos-Ektor Karyotakis, you have been great office mates and I will miss our discussions not only about study, but also about travel experience and philosophy. My sincere thanks go to Yu Ge, Ze Zhang, Yao Cai,

Qian Xun, Constantin Cronrath, and Muhammad Faris who provided invaluable support at the beginning of my doctoral studies. Georg Bökman, Kunal Chelani, and Ida Häggström, I will miss our hiking trips and look forward to more trips like those in the future. Erik Börve, Erik Brorsson, Sondre Chanon Wiersdalen, Daniel Poposki, Palash Gaikwad, Francesco Popolizio, Benedick Allan Strugnell-Lees, Godwin Kwadwo Peprah, and Albert Skegro, I wish you all the best with your remaining PhD journeys! Moreover, I want to thank Dr. David Steen who connected me with other PhD students in the electric power engineering division when I was a teaching assistant in his course. I also want to thank Prof. Erik Agrell for the constructive discussion at the yearly follow-up meetings. In particular, I want to thank our administrator, Christine Johansson, for helping with my onboarding, Chalmers computer, etc.

Last but not least, I owe a great deal to my partner Xixi Liu. You have not only "co-supervised" my doctoral studies but also encouraged me in moments of self-doubt. Without your belief in me, this accomplishment would not have been possible. Thank you for being my partner in life and every step of this academic pursuit! I also want to express my gratitude to my friends, Yang Su, Kun Xiong, and Siyue Zhang for their encouragement and invaluable advice, which was essential to starting my doctoral studies. All the best for your academic or industrial career! Finally, I want to thank my parents for respecting my life decisions since childhood.

Acronyms

BESS:	Battery Energy Storage System
BEV:	Battery Electric Vehicle
BMS:	Battery Management System
CEI:	Cathode Electrolyte Interphase
DEC:	Diethyl Carbonate
DFN:	Doyle-Fuller-Newman
DMC:	Dimethyl Carbonate
DoD:	Depth of Discharge
DVA:	Differential Voltage Analysis
EC:	Ethylene Carbonate
ECM:	Equivalent Circuit Model
EFC:	Equivalent Full Cycle
EIS:	Electrochemical Impedance Spectroscopy
EMC:	Ethyl Methyl Carbonate
EoL:	End of Life
EV:	Electric Vehicle
HEV:	Hybrid Electric Vehicle
ICA:	Incremental Capacity Analysis
LAM:	Loss of Active Material
LCO:	Lithium Cobalt Oxide
LFP:	Lithium Iron Phosphate

LLI:	Loss of Lithium Inventory
LMO:	Lithium Manganese Oxide
LTO:	Lithium Titanate
ML:	Machine Learning
MPC:	Model Predictive Control
MSC:	Maximizing Self-Consumption
NCA:	Lithium Nickel Cobalt Aluminum Oxide
NMC:	Lithium Nickel Manganese Cobalt Oxide
OCP:	Open Circuit Potential
OCV:	Open Circuit Voltage
PBM:	Physics-Based Model
PC:	Propylene Carbonate
PHEV:	Plug-in Hybrid Electric Vehicle
PIML:	Physics-Informed Machine Learning
PINN:	Physics-Informed Neural Network
P2D:	Pseudo-two-Dimensional
pSEI:	Positive Solid Electrolyte Interphase
QRF:	Quantile Regression Forests
RL:	Reinforcement Learning
RPT:	Reference Performance Test
RES:	Renewable Energy Source
SEI:	Solid Electrolyte Interphase
SoC:	State of Charge

SoF:	State of Function
SoH:	State of Health
SoP:	State of Power
SPM:	Single Particle Model
ToU:	Time-of-Use

Contents

Part I

Overview

CHAPTER 1

Introduction

1.1 Motivation

With ever-growing energy demand, many countries worldwide face severe challenges in supplying energy and reducing its resulting carbon dioxide (CO_2) emission. In particular, the transportation and power sectors contribute the largest to the global CO_2 emissions, approximately 62% [1]. Electric vehicles (EVs), as well as renewable energy sources (RESs), are pivotal to reducing global CO_2 emissions [2]. Despite supply chain disruptions, geopolitical uncertainty, and high energy prices, approximately 14 million electric cars (including battery electric vehicles (BEVs) and plug-in hybrid electric vehicles (PHEVs)), 50,000 electric buses, 54,000 electric trucks were sold worldwide in 2023 [3]. An increasing number of EV batteries will be retired after they reach the end of their first lives in vehicles (typically 70-80% of initial nominal capacity) [4]. At the same time, the increasing penetration of RESs into power grids requires urgent solutions to the variable electricity generation resulting from the intermittent nature of RESs [5]. In this regard, stationary battery energy storage systems (BESSs) have become a promising solution thanks to their advantages, such as rapid response, good scalability, and high

round-trip efficiency [5]. A promising scenario is to repurpose EV batteries for second-life applications in stationary BESSs at a good time to maximize the overall value of EV batteries before eventually being recycled. From an economic perspective, this life-sharing scenario may generate extra revenue, which can reduce EV prices further and therefore facilitate EV market adoption [6]. From a technical perspective, shared BESS technology can harmonize the supply chain, production planning, and aftermarket services between EV and stationary manufacturers. From an environmental perspective, repurposing EV batteries for second-life applications can reduce the need for the production of new batteries as well as its resulting CO_2 emissions [7]. However, safe and optimal usage of stationary BESSs based on new and used EV batteries still faces challenges, particularly concerning decision-making under uncertainty across all the life stages of a battery.

In short, second-life applications of EV batteries in BESSs will arguably have enormous economic, technical, and environmental benefits. Lithium-ion battery technology is critical for EV market adoption and RESs grid integration and will continue to play an essential role in second-life BESS market adoption. Other important factors, such as information regarding battery health and lifetime, cost of adaptation at the repurposing stage, requirements of various second-life applications, and the forecasts of relevant markets, must be considered as well for safe and optimal usage of EV batteries in second-life applications. In this thesis, our overarching goal is to enable successful market adoption of second-life BESSs through aging-aware classification and optimal usage of EV batteries. To achieve our goal, we have addressed four research problems in the fields of lithium-ion battery technology, battery management, and system optimization with battery storage. The four research problems are

- Battery lifetime early prediction.
- Battery capacity knee identification and knee-onset early prediction.
- Battery degradation mode estimation and phase detection.
- Energy management in grid-connected microgrids.

1.2 Contributions

To attain our goal by addressing these four research problems, seven research works have been conducted in this thesis. The **key results and main contributions** are as follows:

- To provide battery lifetime early prediction, the quantile regression forests (QRF) model was introduced thanks to its advantages, such as no prior assumption of any specific distribution of battery lifetime, point prediction with high accuracy, and uncertainty quantification as the width of prediction intervals. The learned QRF model was then used to select the high-cycle-life fast-charging protocol (see Paper A).

- To interpret the learned QRF model for battery lifetime early prediction, two model-agnostic interpretation techniques, permutation importance and partial dependence plot, were employed to first rank input feature importance and then quantitatively show the marginal effect that each feature has on the predicted battery cycle life. These two model-agnostic interpretation techniques can be used to study the sensitivity of model output to input perturbations (see Paper A).

- To streamline battery capacity estimation and lifetime prediction model development, a scenario-aware machine learning (ML) pipeline was proposed to automate the process of selecting a feature set for developing the best model in a chosen scenario. The proposed pipeline has advantages, such as scenario-aware battery classification and stratified train-test split (see papers B and C).

- To identify knee and knee-onset points on the battery capacity fade curve, a curvature-based identification method was proposed to first approximate capacity fade curvature and then identify knee and knee-onset points using a time series segmentation algorithm. A new oscillatory degradation phenomenon was discovered and used to divide the battery degradation process into three degradation phases (see Paper D).

- To enable online classification of EV batteries, a transfer learning-based physics-informed framework was proposed to first estimate battery degradation modes and then detect the degradation phase using aggregated

time-series voltage data. Other advanced battery management functions, such as online degradation diagnosis and second-life repurposing, will also become possible in the battery digital twin (see Paper E).

- To enable optimal usage of EV batteries in second-life applications, an economically motivated stage cost function was proposed to account for both the grid and the battery degradation cost in grid-connected microgrids (see Paper F), and an automatic kernel search method was extended with a new base kernel and model selection criteria to construct the best composite kernel in Gaussian process (GP) regression models for battery capacity estimation and residual load prediction in grid-connected microgrids (see Paper G). The proposed cost function and extended GP kernel search method will be used in our future work.

1.3 Thesis Outline

This thesis is divided into two parts, Part I and Part II. Part I consists of six chapters and serves as an introduction to Part II. Specifically about Part I, Chapter 1 provides background and motivation for our goal and states key results and main contributions by addressing four research problems in this thesis; Chapter 2 introduces lithium-ion batteries; Chapter 3 reviews open-source battery datasets and battery models; Chapter 4 describes research problems, and reviews state-of-the-art methods in the literature; Chapter 5 summarizes the included papers from Part II; Chapter 6 concludes Part I and recommends future research directions.

CHAPTER 2

Lithium-Ion Batteries

Since the commercialization of lithium-ion batteries, significant efforts have been made to increase energy density, reduce cost, enhance safety, and improve lifetime and performance [8]. The advances in lithium-ion battery technology make them the exclusive energy sources for the propulsion of battery electric vehicles (BEVs), hybrid electric vehicles (HEVs), and plug-in hybrid electric vehicles (PHEVs). Four aspects of lithium-ion batteries will be discussed in this chapter, i.e., cell materials, cell characterization tests, degradation mechanisms and modes, and capacity knee pathways.

2.1 Cell Materials

The lithium-ion battery cell mainly consists of four components [9]:

- The anode (or negative electrode): The reducing electrode that releases electrons to the external circuit and undergoes oxidation during the electrochemical reaction (discharge).
- The cathode (or positive electrode): The oxidizing electrode that accepts electrons from the external circuit and undergoes reduction during the

electrochemical reaction (discharge).

- The electrolyte: The ionic conductor that provides the medium for the transfer of ions between the negative and positive electrodes inside the cell and is an additional source of lithium ions.
- The separator: A porous membrane placed between the negative and positive electrodes to prevent short circuits while allowing ions to migrate through.

Note that two current collectors are in contact with the two electrodes. The electrochemical reaction of a cell during discharge is illustrated in Fig. 2.1. Specifically, lithium ions are de-intercalated from the anode material, migrate to the surface of the cathode through the separator and electrolyte, and then insert into the cathode material. The charge process is the same process, but reversed.

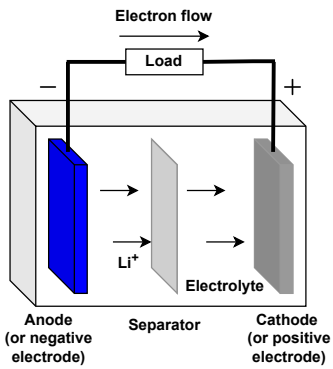

Figure 2.1: Schematic illustration of a cell during discharge [9].

Anode Materials

Currently, state-of-the-art negative electrode materials used in lithium-ion batteries are synthetic and artificial graphites, natural graphites, and amorphous carbons [10]. Synthetic and artificial graphites are the most commonly

used negative electrode materials in EVs due to their high levels of purity and consistent quality [11]. A small amount of silicon is also added to the anode in some commercial cells in order to increase cell energy further [10]. Lithium titanate (LTO) is used in some commercial cells, which makes these cells more suitable for power applications, such as in hybrid electric heavy-duty vehicles [12]. Lastly, lithium metal is considered as an ideal anode material for applications, especially in all-solid-state batteries that utilize ceramic or polymetric electrolytes. However, it suffers from several issues, such as dendrite growth, unstable reaction interface, volume change, and low Coulombic efficiency [13].

Cathode Materials

The cathode has been a bottleneck in terms of specific capacity since the commercialization of lithium-ion batteries. It is typically a lithium transition metal oxide material capable of reversible delithiation of lithium ions [14]. The most widely used positive electrode materials in EVs are lithium nickel manganese cobalt oxide (NMC), lithium manganese oxide (LMO), lithium nickel cobalt aluminum oxide (NCA), and lithium iron phosphate (LFP) [11]. Fig. 2.2 illustrates the energy density versus the specific energy of different cell chemistries at the positive electrode. Generally, a higher amount of Ni content implies a higher capacity. Therefore, a commonly employed strategy to maximize the energy content of NMC cathodes is to maximize the Ni content [15]. With outstanding rate capability at an affordable price, LMO is often blended with Ni-rich layered cathodes with the aim of increasing power density and safety [11]. While reducing the LMO content in cathode material blends will improve energy density further [11]. Currently, the state-of-the-art cathode materials are NCA which has the advantage of capacity retention, along with NMC 532, NMC 622, and NMC 811 [11]. Despite the relatively low volumetric capacity of LFP, its robustness offers a promising prospect in heavy-duty vehicle applications like buses and trucks, where its extended cycle life and excellent rate capability become advantageous [11].

Electrolytes

Commercial lithium-ion batteries generally contain liquid electrolytes mainly composed of solvents, lithium salt, and additives, which are combined in specific proportions under controlled conditions to meet desired characteristics

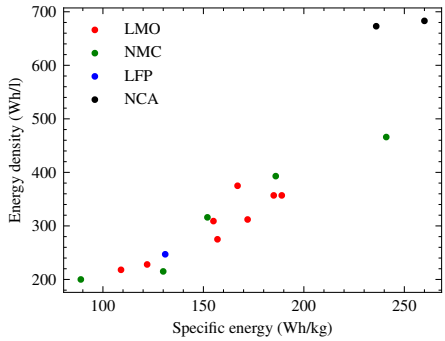

Figure 2.2: Energy density versus specific energy of different cell chemistries at the positive electrode [11].

[16]. The solid electrolytes that function as both a separator and an electrolyte are considered safer than the conventional setup of a separator and a liquid organic electrolyte [17]. Therefore, solid electrolytes are gaining more and more attention. However, major challenges such as high production costs remain to be overcome by technology breakthroughs [17].

Separators

If a liquid electrolyte is employed in a lithium-ion battery cell, it will be essential to place a porous membrane sandwiched between the positive and negative electrodes to prevent physical and electrical contact between the electrodes while permitting ion transport [18]. The characteristics of separators, such as porosity, pore size, electrolyte affinity, mechanical strength, and melting point, have an impact on the ion transport, lifetime, performance, and safety of lithium-ion batteries [18]. Currently, three main types of separators are available, which vary in terms of chemistry and production process, i.e., microporous polyolefin separators, nonwoven separators, and ceramic composite separators [18]. State-of-the-art polyolefin separators have been widely adopted in commercial lithium-ion batteries. However, low electrolyte affinity and low thermal stability are their major limitations [18].

2.2 Cell Characterization Tests

The continuous advances in lithium-ion battery technology (e.g., new electrode material, cell design, and manufacture) motivate the need for non-invasive cell characterization tests in the lab, in which three parameters are typically measured, i.e., capacity, internal resistance/impedance, and open circuit voltage (OCV) [19]. These tests can be used for both characterizing initial cell performance and tracking the evolution of cell performance (i.e., cell degradation) through reference performance tests (RPTs) [20]. Notably, there are different ways of conducting characterization tests, and consequently, capacity, resistance, and OCV measurements may vary from one to another depending on the specific experimental setup.

Capacity Tests

Depending on ambient temperature and charge-discharge C-rate, the measured capacity of the same cell can be different, which captures different degradation information. Note that C-rate is defined as the current value which discharges a battery from a fully charged state to a fully discharged state in one hour [19]. Lower C-rates ($\leq$ C/10) provide thermodynamic information through loss of lithium inventory (LLI) and loss of active material (LAM), which enables incremental capacity analysis (ICA) [21] and differential voltage analysis (DVA) [22]. Higher C-rates ($\geq$ C/10) provide a combination of both thermodynamic information and kinetic information through impedance growth.

The experimental data obtained from constant-current capacity tests can be used for two purposes, i.e., modeling the battery degradation process using physics-based models, (semi-)empirical models, or machine learning models; understanding the causal relationship between battery usage profile (e.g., static cycling aging, dynamic cycling aging, storage aging) and capacity fade.

Internal Resistance/Impedance Tests

Intrinsically, the power capability of a battery cell is associated with its impedance characteristics. The impedance of a cell determines the voltage response to a given current load, characterized by its amplitude, frequency, and time duration [19]. The resistive part (i.e., the real part of the complex

impedance) directly contributes to the dissipative heat generation of a cell, and the resulting cell temperature increase while in use [23]. Moreover, the resistive part consists of pure ohmic resistance, charge transfer resistance, and entropy change [19]. Therefore, the cooling system design mainly depends on the resistive values of cell impedance.

Two well-established cell impedance measurement techniques are introduced here.

Pulse Power Tests

The pulse power tests were initially proposed by the United States Advanced Battery Consortium (USABC) [24], and are also known as hybrid pulse power characterization (HPPC). The tests measure the voltage response to a square-wave current load that is applied to a cell. The resistance is then obtained as the ratio of the measured voltage response to the applied current, which consists of three parts, i.e., ohmic resistance, charge transfer resistance, and polarization resistance [19]. The experimental data obtained from pulse power tests can be utilized to parameterize equivalent circuit models (ECMs) that are used to estimate the state of power (SoP) [25], and state of charge (SoC) of a cell [26]. Moreover, pulse power tests have also been employed to parameterize cell electro-thermal models [27], and characterize cell degradation through resistance rise [28].

Electrochemical Impedance Spectroscopy Tests

Electrochemical impedance spectroscopy (EIS) tests were introduced to investigate the electrochemical behavior of a cell over a wide range of frequencies [19]. In EIS tests, a small amplitude sinusoidal potential as input stimulus is applied to an electrochemical cell. As a result, the current response in a linear or pseudo-linear system is a sinusoid with the same frequency but with a different amplitude and a phase shift relative to the input. The current response and the input voltage are then used to calculate the impedance of the cell in the frequency domain. The impedance spectrum of a cell is typically represented by a Nyquist plot that consists of the real and imaginary parts of the impedance. The experimental data obtained from EIS tests can be used to characterize the electrochemical dynamics of a cell [29], estimate cell temperature [30], parameterize ECMs [31], and identify cell degradation

mechanisms [32] [33].

Open Circuit Voltage Tests

OCV tests measure the equilibrium voltage of a cell as a function of the SoC. At the cell level, the OCV curve is defined by open circuit potential (OCP) curves of two electrodes, the loading ratio between two electrodes, and an SoC offset between two electrodes [34], while at the electrode level, the OCP curve is defined as the potential difference between the electrode and the reference [35]. An example of the impact of changes of loading ratio and SoC offset on capacity loss is given in Ref. [19].

To understand the OCV curves, the definition of SoC is of equal importance. However, the definition of SoC in the literature varies from one to another. There are mainly three different SoC definitions in the literature, which are listed as follows:

- USABC definition [24]: "The ratio of the Ampere hours remaining in a cell at a given rate to the rated capacity under the same specified conditions".

- Thermodynamic definition [19]: "The ratio of the remaining intercalation sites for lithium ions divided by the total number of sites".

- Low-rate definition [36]: "The ratio of the remaining exchangeable lithium ions to the maximum number of exchangeable lithium ions at a low rate (e.g., C/25) for a given potential window".

Both USABC and thermodynamic definitions depend on the application and cannot be adapted to cells and packs nowadays, but the low-rate definition is generally applicable to half-cells, full-cells, and battery packs.

Two commonly used OCV measurement techniques are introduced here.

Galvanostatic Intermittent Titration Technique

One test procedure is proposed by USABC, i.e., after resting for one hour, the cell is discharged at 10% SoC increments and the voltage is recorded [37]. More accurate measurements of OCV can be achieved by reducing the SoC increments to less than 10% and increasing rest periods to longer than one

hour [19]. However, to avoid prohibitively long test time, there is a trade-off between the accuracy of OCV measurements and the cost of longer rest periods and shorter SoC increments. The OCV curves obtained from GITT tests can be used to characterize cell performance (e.g., rate capabilities of a cell [38]), study OCV hysteresis of different chemistries [39], parameterize OCV models [35] and ECMs [40], and identify degradation mechanisms [41].

Pseudo-OCV Tests

Depending on the required accuracy of OCV measurements, the long test time of a GITT test may hinder its wide adoption in battery studies. In this regard, pseudo-OCV provides an alternative solution to obtain OCV curves with significantly less time, i.e., cycling a cell at a low charge and discharge rate (typically $\leq$ C/25) and then averaging the charge and discharge curve in order to address the cell hysteresis and polarization issue [21] [42]. The reason for the low current rate is to reduce the kinetic effects, electrode polarization, and heat generation due to ohmic resistance. The OCV curves obtained from pseudo-OCV tests can be used to identify and quantify degradation modes after taking their derivatives (e.g., incremental capacity analysis [21], differential voltage analysis [22]), improve model-based voltage estimation accuracy by including hysteresis effects [43], and estimate SoC [44].

2.3 Degradation Mechanisms and Modes

As a result of an intricate interplay of various mechanical and chemical degradation mechanisms, the performance of lithium-ion battery cells degrades, for example, cell capacity fades, and cell resistance/impedance rises. Inside the cell, degradation mechanisms occur in different components, i.e., the anode, the cathode, the electrolyte, the separator, and the current collectors [14] [45] [46]. Considering the influence of the electrolyte and its own degradation, which mainly occurs in interaction with the electrodes, the degradation mechanisms of the cell are therefore discussed separately at the anode and cathode.

Degradation Mechanisms at the Anode

Graphite, an allotrope of carbon, is the primary material used for anodes in lithium-ion battery cells (see Subsection 2.1). As a result, degradation mechanisms at the graphite anode have been better studied than those at the cathode in the literature. However, it is generally difficult to generalize those degradation mechanisms that have been reported in the literature as each lithium-ion battery cell has its own cell design (e.g., chemistry and geometry) [34] and manufacture [47], which intrinsically has an impact on the cell degradation. Therefore, only the dominant degradation mechanisms at the anode are listed as follows [14] [45]:

- Solid electrolyte interphase (SEI) growth.
- SEI decomposition.
- Electrolyte decomposition.
- Binder decomposition.
- Graphite exfoliation.
- Lithium plating/dendrite formation.
- Loss of electric contact.
- Electrode particle cracking.
- Corrosion of current collector.

Degradation Mechanisms at the Cathode

Similarly, cathode materials (see Subsection 2.1) significantly impact the performance of lithium-ion battery cells. In the literature, lithium manganese oxides with spinel structure and lithium nickel cobalt mixed oxides with layered structures have been intensively studied. The dominant degradation mechanisms at the cathode of these materials are listed as follows [14] [45]:

- Electrolyte decomposition.
- Binder decomposition.

- Loss of electric contact.
- Corrosion of current collector.
- Structural disordering.
- Electrode particle cracking.
- Transition metal dissolution/dendrite formation;
- Cathode electrolyte interphase (CEI) (or positive solid electrolyte interface (pSEI)) growth.

Degradation Modes

The dominant degradation mechanisms occurring at the anode or the cathode are clustered into three degradation modes which have unique and quantifiable effects on the OCV of lithium-ion cells and electrodes [46]. The three degradation modes are as follows:

- Loss of lithium inventory (LLI);
- Loss of active material at the negative electrode ($\mathrm{LAM_{NE}}$);
- Loss of active material at the positive electrode ($\mathrm{LAM_{PE}}$).

The directly observable effects of these degradation mechanisms are capacity fade and power fade as illustrated in Fig. 2.3. Capacity fade is a reduction in the usable capacity of the cell and power fade is a reduction of the deliverable power of the cell [14].

Interactions Between Degradation Mechanisms

The interactions between different degradation mechanisms and modes result in positive and negative feedback loops [14] [48].

- Positive feedback: For example, SEI growth can decrease porosity and result in high electrolyte potentials near the NE-separator interface, leading to lithium plating [14]; particle cracking during cycling can create new surfaces and accelerate SEI growth and lithium plating [48]; particle cracking can also be self-reinforced via increased current density on

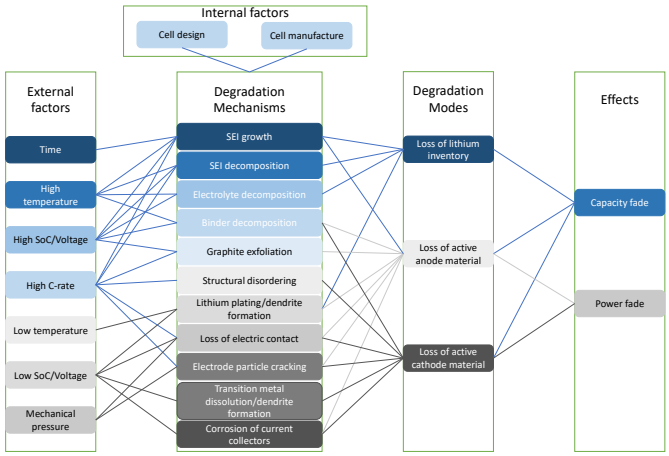

Figure 2.3: Cause and effect of dominant degradation mechanisms and their associated degradation modes [34] [45] [46].

the remaining active area [49]; lithium plating can also be self-reinforced via pore blockage [50]; transition metal dissolution at the cathode has been found to accelerate SEI growth [51]; transition metal dissolution and migration into the cathode can lead to a reduced lithium diffusivity, which can lead to more severe concentration gradients and accelerated particle cracking [14].

- Negative feedback: For example, SEI formation prevents further electrolyte decomposition [52], SEI growth causes LLI, which increases the anode potential that limits lithium plating [48] [49].

2.4 Capacity Knee Pathways

In some experimental tests, lithium-ion batteries can exhibit a two-stage capacity fade behavior, with a slow degradation rate in the first stage, and then an accelerated degradation rate in the second stage [34] [53] [54]. The transition from the first stage to the second stage forms a knee shape on the capacity fade curve. The knee occurrence not only severely shortens battery lifetime but also poses potential safety issues [55]. Therefore, for profitability

and safety reasons, the occurrence of the knee should be avoided, or at least delayed.

In this section, we summarize three common knee pathways from the literature, i.e., lithium plating-induced, resistance growth-induced, and mechanical deformation-induced. For a comprehensive review of knee pathways, the author kindly refers readers to Ref. [56]. Each knee pathway may consist of one or multiple internal state (degradation mechanism or degradation mode) trajectories that lead to a knee, and each degradation mode may be contributed by multiple degradation mechanisms (see Subsection 2.3 2.3) and their interactions 2.3. Although it can be challenging to identify or experimentally isolate degradation mechanisms, degradation modes are identifiable through OCV measurements and their derivatives [46], which can be used for validating a knee pathway.

Lithium Plating-Induced Knee Pathways

Lithium plating takes place when lithium ions form metallic lithium on the surface of the electrode instead of intercalating into it. The lithium plating is favorable over intercalation when the reaction potential of Li/Li^+ is greater than the local electrode potential. Lithium plating can occur in either fresh cells or aged cells, and be either rate-dependent (i.e., plating occurs if the applied current exceeds a threshold) or rate-independent (i.e., plating occurs regardless of the applied current rate) [56]. Moreover, lithium plating can occur with various degrees of reversibility within a cycle, which is defined as the ratio of lithium that is plated during charge and subsequently stripped to the electrolyte during discharge [57] [58].

Historically, lithium plating has been considered to be the primary degradation mechanism that accounts for knee occurrence on the capacity fade curve. In this subsection, we explore the degradation mechanisms and pathways through which plating can result in the formation of a knee.

- Rate-dependent lithium plating: Rate-dependent lithium plating occurs when the reaction potential of Li/Li^+ is greater than the local electrode potential [56].
  - Rate-dependent lithium plating in fresh cells can be caused by high charge C-rate, low temperature, or high mechanical stress [56]. Higher temperature [59], thinner electrode design [60], and optimal

design of charging protocols [61] can significantly extend battery lifetime by avoiding or delaying rate-dependent lithium plating in fresh cells.

  - Rate-dependent lithium plating in aged cells can be caused by loss of active material of the delithiated negative electrode ($\mathrm{LAM_{deNE}}$). Specifically, the loss of active material without a corresponding loss of lithium flux will lead to increased local current density on the surface of the negative electrode, which can drive higher overpotentials and resulting lithium plating. In principle, loss of active material of the delithiated negative electrode ($\mathrm{LAM_{deNE}}$) can be caused by various degradation mechanisms in parallel (see Fig. 2.3), for example, graphite exfoliation, electrode particle cracking. The major challenge of identifying and quantifying $\mathrm{LAM_{deNE}}$ is to combine the rate-independent estimate from low-rate cycling data with the rate-dependent kinetic effects.
  - Rate-dependent lithium plating in aged cells can also be caused by SEI growth. Specifically, SEI growth can lead to rated-dependent lithium plating in two ways, i.e., by decreasing the porosity of the negative electrode and the resulting electrolyte transport kinetics, or by decreasing the charge-transfer kinetics of the negative electrode particles. Tracking the negative electrode porosity [62] and the charge-transfer kinetics [63] over life can be performed via EIS (see Subsubsection 2.2). However, identifying the critical porosity threshold or the critical charge-transfer kinetics threshold at which rate-dependent lithium plating starts is challenging and requires accurate electrochemical modeling of the porous electrode.

- Rate-independent lithium plating: Rate-independent lithium plating occurs whenever the negative electrode is not able to accommodate all the lithium from the positive electrode during charge [56].
  - Rate-independent lithium plating in fresh cells can be caused by low ratios of negative electrode capacity to positive electrode capacity (i.e., $n : p < 1$). The capacity knee due to rate-independent lithium plating in fresh cells often occurs in the early life of a cell, which can be easily avoided by improving cell design [64]. Considering that the loading ratios are often provided as a part of cell design in-

formation, modeling, identifying, and predicting rate-independent lithium plating in fresh cells becomes trivial.

– In contrast, rate-independent lithium plating in aged cells can be caused by loss of active material of the delithiated negative electrode (LAM_{deNE}). Specifically, if the negative electrode capacity falls below the remaining lithium inventory in a cell, the negative electrode will not be able to accommodate all the lithium from the positive electrode during charge, which leads to irreversible lithium plating and a resulting LLI. The LAM_{deNE} and LLI together contribute to accelerated capacity fade, at which a knee also occurs. In principle, loss of active material of the delithiated negative electrode (LAM_{deNE}) can be caused by various degradation mechanisms in parallel (see Fig. 2.3), for example, graphite exfoliation, and electrode particle cracking. Although it is challenging to identify or experimentally isolate the exact degradation mechanisms that lead to LAM_{deNE}, LAM is identifiable through OCV measurements and their derivatives [57] [65] [66].

The aforementioned lithium plating-induced knee pathways are illustrated in Fig. 2.4. The lithium plating-induced knees are commonly observed or hypothesized in commercial LFP/graphite cells [61] [65] [66] [67] [68].

Resistance Growth-Induced Knee Pathways

The internal resistance of a cell often increases as it degrades over life, partially due to the growth of side reaction products (e.g., SEI) on the surface of the electrode. With constant current applied, the overpotential due to increased internal resistance will have a cell reach its cutoff voltage more quickly, and therefore decrease its capacity per cycle. Specifically, at higher voltage levels, the voltage-capacity curves of most lithium-ion batteries tend to exhibit a relatively flat pattern, while at lower voltage levels, the curves become relatively steep. Thus, the charge capacity is highly sensitive to small resistance growth, while the discharge capacity is less sensitive to it until the overpotential becomes large enough so that the discharge stops within the flat region of the voltage-capacity curves. Then it will lead to a capacity knee. This resistance growth knee pathway is not only sensitive to electrode chemistry as each chemistry has its own voltage-capacity curve, but also the discharge

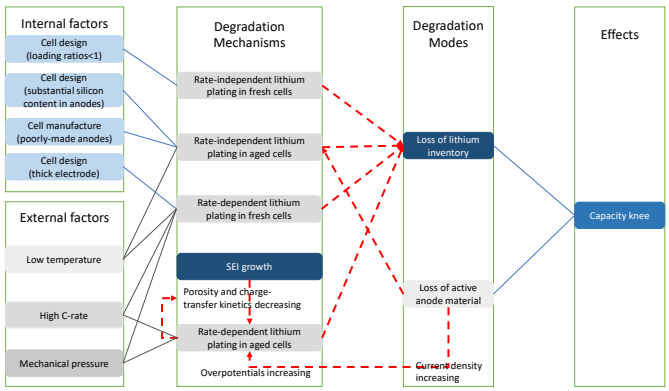

Figure 2.4: Lithium plating-induced knee pathways [56]. Note that dashed red lines indicate the interactions between degradation mechanisms and modes.

C-rate and lower cutoff voltage that vary widely in the field [56].

The resistance-growth knees are commonly observed or hypothesized in cells made of oxide-based cathode materials (see Subsection 2.1) such as NMC as they often operate above the stability window of the electrolyte [69] [70].

Mechanical Deformation-Induced Knee Pathways

Mechanical degradation mechanisms that occur over multiple length scales, i.e., at the micro-scale (particle level), meso-scale (component level), and macro-scale (cell level), can form pathways for knees [56]. Moreover, these effects often interact in positive feedback loops and are closely related to other knee pathways, for example, lithium plating knee pathways [47].

- At the micro-scale: The intercalation and deintercalation of lithium can stress electrode particles, which can lead to both loss of active material and accelerated SEI at the anode and CEI (or pSEI) growth at the cathode through particle cracking [48]. The positive feedback loop between loss of active material and particle cracking can lead to a knee [49].

- At the meso-scale: The growth of covering layers on the surface of the negative electrode at the interface with the separator is commonly observed in cylindrical cells with knee occurrence [67] [71], which leads to loss of active material and lithium plating.
- At the macro-scale: Different mechanical deformation occurs depending on the form factor of a cell. For example, jelly roll deformation has been identified in cylindrical cells with knee occurrence [72] [73]; external pressure can shorten cell lifetime via knee occurrence in both pouch and prismatic cells [74].

The mechanical deformation-induced knee pathways over multiple length scales are illustrated in Fig. 2.5. The mechanical deformation-induced knees have been observed or hypothesized in cells with their cathode made of NMC [72] and NCA [75].

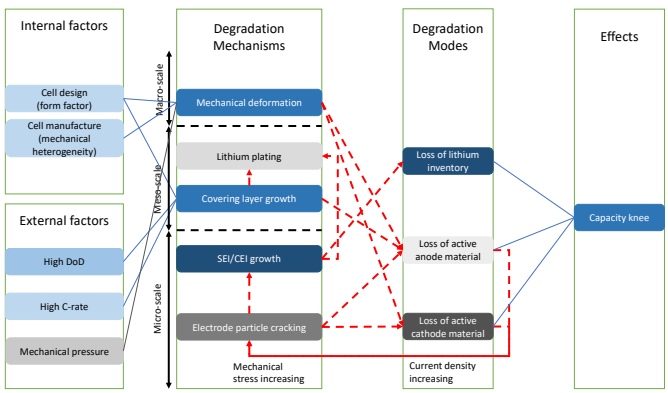

Figure 2.5: Mechanical deformation-induced knee pathways [56]. Note that dashed red lines indicate the interactions between degradation mechanisms and modes.

CHAPTER 3

Battery Datasets and Models

This chapter summarizes open-source battery datasets used in this thesis and reviews battery models that directly or indirectly characterize degradation behaviors in various applications. Lastly, a scenario-aware machine learning pipeline is introduced for model development in a chosen scenario.

3.1 Open-Source Battery Data

Acquiring high-quality battery data in the laboratory can be time-consuming and expensive. Nevertheless, researchers rely on these data to parameterize and validate battery models that characterize different battery behaviors. As illustrated in Fig. 3.1, time-series usage data is continuously measured through aging tests, such as voltage, current, and cell temperature, while characterization data is periodically measured through reference performance tests (RPTs), such as capacity, internal resistance/impedance, and open circuit voltage (OCV). Furthermore, battery load profiles in aging tests can be classified into three categories [76]:

- Identical cycling scenario: Batteries are cycled repeatedly under iden-

tical or nearly identical conditions to quantify their intrinsic cell-to-cell variations, such as battery capacity, internal resistance, and lifetime spreads.

- Protocol cycling scenario: Batteries are cycled repeatedly under various cycling protocols to characterize the impact of different protocols (e.g., formation protocols or fast-charging protocols) or stress factors (e.g., ambient temperature, charge and discharge C-rates, depth-of-discharge (DoD), average state-of-charge (SoC)) on battery health degradation and lifetime.
- Dynamic cycling scenario: Batteries are cycled repeatedly under application-specific load profiles to characterize battery aging in real-world applications.

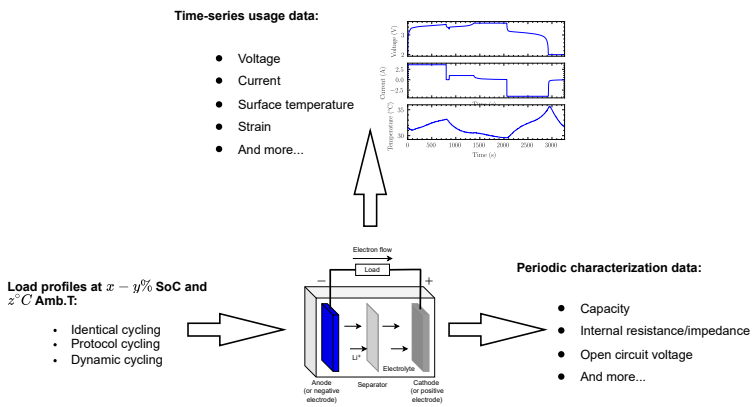

Figure 3.1: Lithium-ion battery aging tests.

In recent years, large amounts of battery data of different technologies (nominal capacity, chemistry, form factor, etc.) have been generated under well-controlled operating conditions in the laboratory and realistic operating conditions in the field (see Fig. 3.2). We therefore resort to open-source battery datasets to make transparent and reproducible research contributions at minimum costs. In total, five open-source battery datasets have been used in this thesis and will be described in the following subsections.

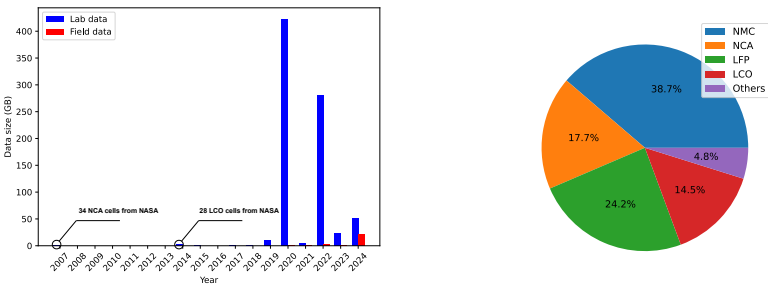

(a) The trend of battery data with size measured in GB.

(b) The categorization of battery data based on chemistry.

Figure 3.2: The open-source lithium-ion battery data generated in the lab and field [77] [78].

Toyota Research Institute Dataset

The first battery dataset was generated by Toyota Research Institute in partnership with Stanford University and Massachusetts Institute of Technology [61] [66]. This dataset has 169 lithium iron ferrous phosphate (LFP)/graphite cylindrical cells manufactured by A123 Systems (model APR18650M1A, 1.1 Ah nominal capacity). The test purpose is to characterize the impact of various fast-charging protocols on battery health degradation and then select the high-cycle-life fast-charging protocol. All the cells were charged with one of one-step or multi-step charging protocols from 0% to 80% SoC, and then charged with a uniform 1C constant current–constant voltage (CC-CV) charging step from 80% to 100% SoC. Subsequently, all the cells were identically discharged with a 4C CC-CV discharging step to 0% SoC. All the cells were tested in an environmental chamber at a constant temperature of 30°C. The cells were cycled until they reached the end of life (EoL) threshold, defined as 80% of initial nominal capacity in this dataset. Time-series cell voltage, current, and (surface) temperature in each cycle were continuously measured, while two battery health metrics, i.e., capacity (4C discharge, 30°C) and internal resistance (±3.6C pulse current, 30 or 33 ms pulse width, 80% SoC) were measured per cycle.

All the cells in this dataset have knee occurrence on their capacity fade

curves before the end of the experiment (see Fig. 3.3).

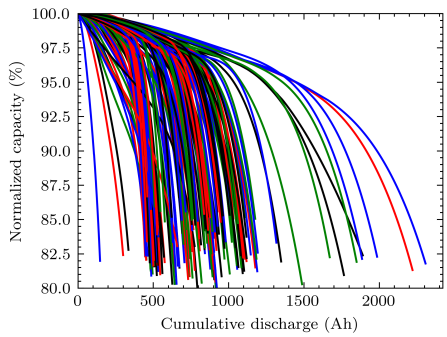

Figure 3.3: Normalized capacity fade curves of LFP/graphite cells in the Toyota Research Institute dataset [61] [66].

The knee occurrence is caused by lithium plating due to loss of active material of the delithiated negative electrode (LAM_{deNE}) (see Subsection 2.4). Specifically, at high rates of LAM_{deNE}, the negative electrode capacity eventually falls below the remaining lithium inventory in a cell. Then, the negative electrode will not be able to accommodate all the lithium from the positive electrode during charge, which leads to irreversible lithium plating and the resulting loss of lithium inventory (LLI). The LAM_{deNE}, together with LLI, contribute to accelerated capacity fade, at which a knee also occurs. Moreover, a higher charge C-rate also accelerates the occurrence of the knee.

Sandia National Lab Dataset

The second battery dataset was generated by Sandia National Laboratories [70], which has 32 lithium nickel manganese cobalt oxide (NMC 811)/graphite cylindrical cells manufactured by LG Chem (model 18650HG2, 3 Ah nominal capacity). The test purpose is to characterize the impact of three stress factors, i.e., ambient temperature, DoD, and discharge C-rate, on battery health degradation. All the cells were identically charged at a 0.5C rate, and to probe a wide range of parameter space, the cells were cycled at three different ambient temperatures (15°C, 25°C, and 35°C) with different DoD (40-60%, 20-80%, and 0-100%) and discharge C-rates (0.5C, 1C, 2C, and 3C). The cells were cycled beyond the EoL threshold, i.e., 80% of their initial nominal capac-

ity. Time-series cell voltage, current, and (surface) temperature in each cycle were continuously measured, while one battery health metric, i.e., capacity (0.5C discharge, the same ambient temperature as that in each cycling test) was measured periodically.

Note that 5 cells that were cycled with 20-80% DoD and one cell that was cycled with 0-100% DoD are excluded from this thesis due to the fact that their discharge capacity data is highly corrupted. In the end, 26 cells that have knee occurrence on their capacity fade curves before the end of the experiment are included in this thesis (see Fig. 3.4).

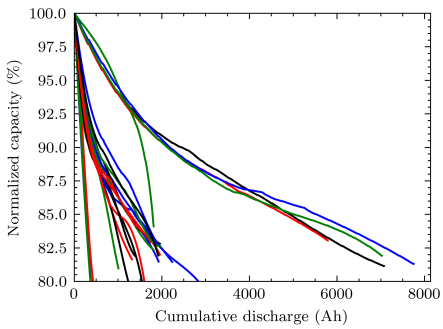

Figure 3.4: Normalized capacity fade curves of NMC/graphite cells in the Sandia National Lab dataset [70].

The knee occurrence is attributed to resistance growth that is caused by the growth of side reaction products (e.g., SEI) on the surface of the electrode (see Subsection 2.4). As illustrated in Fig. 3.5, the NMC/graphite cells in this dataset have discharge voltage-capacity curves that are relatively flat at higher voltage levels and relatively steep at lower voltage levels. At the beginning of life, the discharge ends within the steep region of the voltage-capacity curve. However, as the overpotential increases due to resistance growth during aging, the voltage-capacity curve is pushed downwards. As a result, a cell reaches its lower cutoff voltage more quickly, and the discharge eventually ends within the flat region of the voltage-capacity curve, in which the discharge capacity is highly sensitive to small resistance growth. Then, the discharge capacity fade accelerates assuming a linear resistance growth rate, which leads to a capacity knee.

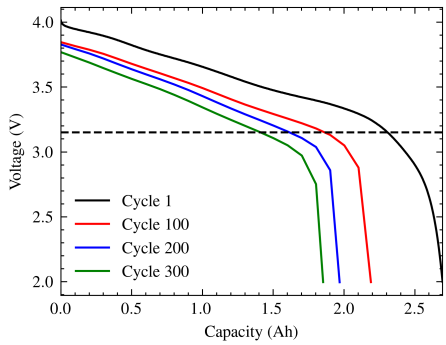

Figure 3.5: Discharge voltage-capacity curve of a sample NMC/graphite cell [No.1] in the Sandia National Lab dataset [70].

Stanford Energy Control Lab Dataset

The third battery dataset was generated by Stanford Energy Control Laboratory [79], which consists of 10 NMC 811/graphite-SiO_x cylindrical cells manufactured by LG Chem (model INR21700-M50T, 4.85 Ah nominal capacity). The test purpose is to characterize battery aging under real-driving profiles. All the cells were first CC charged with one of 4 different C-rates (C/4, C/2, 1C, and 3C) until the voltage reached 4 V, and then CV charged until the current reached the cutoff value of 50 mA. Next, cells were CC-CV charged at C/4 until the voltage reached 4.2 V, corresponding to 100% SoC. Subsequently, cells were identically discharged at C/4 from 100% to 80% SoC, and then discharged with the Urban Dynamometer Driving Schedule (UDDS) driving profile to 20% SoC. All the cells were cycled in an environmental chamber at a constant temperature of 23°C. Unfortunately, none of the cells in this dataset reached the EoL threshold, i.e., 80% of their initial nominal capacity. Time-series cell voltage, current, and (surface) temperature in each cycle were continuously measured, while two battery health metrics, i.e., capacity (C/20 discharge, 23°C), and internal resistance (from Hybrid Pulse Power Characterization tests) were measured every 25 or 50 cycles.

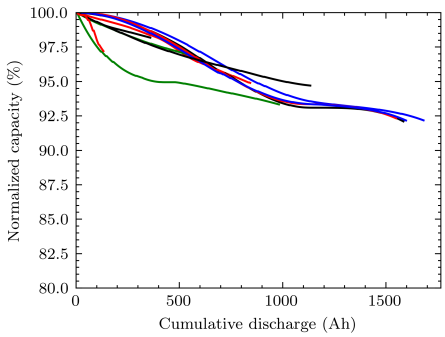

Figure 3.6: Normalized capacity fade curves of NMC/graphite-SiO_x cells in the Stanford Energy Control Lab dataset [79].

Imperial College London Dataset

The fourth battery dataset was generated by Imperial College London [80], which consists of 40 NMC 811/graphite-SiO_x cylindrical cells manufactured by LG Chem (model GBM50T2170, 5 Ah nominal capacity). The test purpose is to characterize battery aging under 15 different operating conditions (i.e., ambient temperature and SoC) and quantify degradation modes. All the cells were charged with a uniform 0.3C CC-CV charging step, and then discharged with a 1C CC discharging step except for one experiment that discharged the cells with the World wide harmonized Light vehicle Test Protocol (WLTP) driving profile. Moreover, the cells were cycled under 3 different ambient temperatures (10°C, 25°C, and 40°C), and 5 different SoC windows (0-30%, 70-85%, 85-100%, 0-100%, and 0-100% with a driving profile). Two battery health metrics, i.e., capacity (C/10 discharge, 25°C), and internal resistance (from Galvanostatic Intermittent Titration Technique) were measured periodically. Moreover, degradation modes of LAM_{NE} and LAM_{PE}, LLI, and graphite as well as silicon active materials at the negative electrode were also estimated using pseudo-OCV data.

In total, 18 cells are included in this thesis (see Fig. 3.7). It can be seen that 6 cells have knee occurrence on their capacity fade curves, which is likely due to lithium plating at the negative electrode and its resulting LLI.

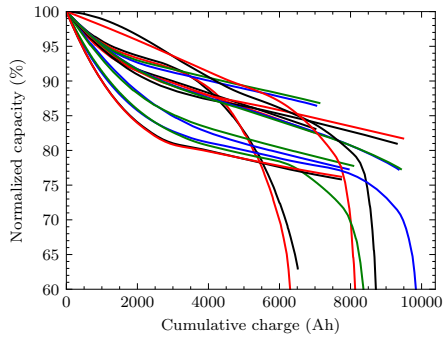

Figure 3.7: Normalized capacity fade curves of NMC/graphite-SiO_x cells in experiment 1, 4 and 5 of Imperial College London dataset [80].

Chalmers University of Technology Dataset

The fifth battery dataset was generated at Chalmers University of Technology [81], which consists of 12 synthetic NMC 811/graphite-SiO_x cylindrical cells (INR21700-M50, 5 Ah nominal capacity). The purpose is to understand interactions between multiple degradation mechanisms and their resulting degradation pathways inside LG M50 cells and to simulate the knee occurrence on the capacity fade curve. Specifically, four degradation mechanisms, i.e., SEI growth, particle cracking, lithium plating, and LAM, were coupled to a Doyle-Fuller-Newman (DFN) model, and three degradation parameters were varied from their default values as parameter sensitivity analysis. In each simulation, all the cells were CC discharged at 1C to 2.5 V and then CV discharged until the current cut-off (50 mA) followed by a rest for 5 minutes. Subsequently, cells were CC charged at 1C to 4.2 V and then CV charged until the current cut-off (50 mA) followed by a rest for another 5 minutes. The ambient temperature was set to be constant at 25°C. In the end, some cells have knees on their capacity fade curves, of which the particle cracking-induced knees were used for validating the effectiveness of our proposed knee-onset and knee identification method in Ref. [82].

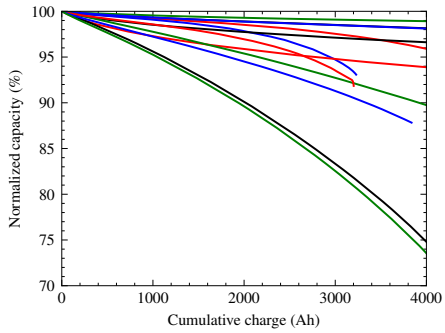

Figure 3.8: Normalized capacity fade curves of synthetic NMC/graphite-SiO_x cells in the Chalmers University of Technology dataset [80].

3.2 Battery Models

Many kinds of battery models have been developed to characterize different battery behaviors on multiple time and length scales, such as electrical, electrochemical, thermal, mechanical, and degradation behaviors. In particular, battery models that directly or indirectly characterize degradation behaviors, such as capacity fade, resistance growth, and degradation mode analysis, can be divided into four categories:

- Physics-based models: Broadly defined, physics-based models include electrochemical models derived from first principles using porous electrode theory (e.g., the pseudo-two-dimensional (P2D) model [83], single particle model (SPM) [84]), physics-based degradation models (e.g., SEI growth models [85] [86], lithium plating models [50] [87] [88], particle cracking models [89] [90], loss of active material models [90] [91], etc.), and the mechanistic model [34].

- (Semi-)empirical models: Empirical or semi-empirical models may be the most commonly used model type to capture the direct relationship between the operating conditions and the battery SoH with affordable computational cost. It is common in the literature that only cycling aging as the function of cycle number, or equivalent full cycle number, or Ah-throughput, is considered in empirical models, such as exponential [53], logarithmic [54], polynomial [92], and hybrid [93] models, while

semi-empirical models often consider both calendar aging and cycling aging with square-root-of-time dependency due to SEI growth [94] and Arrhenius temperature dependency [95]. To develop a (semi-)empirical model for a specific type of lithium-ion cell, relevant stress factors need to be first identified for both calendar aging and cycling aging, for example, storage temperature [96] [97] [98], storage voltage [96], and storage SoC [97] [98] in calendar aging; charge and discharge C-rate [97] [99], average voltage [96], average SoC [97] [98], DoD [96] [98] [99], and ambient temperature [97] [98] [99] in cycling aging. Moreover, equivalent circuit models (ECMs) characterize the electrical behavior of a battery using different combinations of circuit elements, such as resistors and capacitors [100].

- Machine learning models: Generally, machine learning (ML) models for battery applications can be either non-probabilistic or probabilistic. Non-probabilistic machine learning models include autoregression based models [101] [102], elastic net [66], support vector regression [103] [104], random forest regression [105], gradient boosting regression tree [106], long short-term memory [107] [108], and recurrent neural network [109]. Probabilistic machine learning models include Gaussian process regression [110], relevance vector machine [111] [112], quantile regression forest [113], and Bayesian neural network [114].

- Hybrid physics-based and machine learning models: To further improve battery lifetime prediction performance, there has been growing interest in combining physics-based and ML models to leverage their respective advantages, i.e., the flexibility of ML modeling approach and the interpretability of physics-based modeling approach [115]. Broadly, they can be divided into two categories, i.e., sequential integration of standalone physics-based and ML models, and hybridization of physics-based and ML models. Sequential integration can be easily achieved through integrating existing software, while hybridization remains an open challenge in physics-informed machine learning (PIML) [116].

A comparison of commonly used lithium-ion battery models (P2D, SPM, ECM, and PIML) in accuracy, computation time, and interpretability is illustrated in Fig. 3.9. The P2D model provides insights into the internal dynamics of a battery with the highest accuracy but requires the highest computational

time. In contrast, the ECM model has the lowest computational time but the accuracy is restricted to the range that the model has been parameterized. The PIML model may provide a good trade-off between accuracy and computational time/interpretability. We will discuss the different approaches for enforcing physics into ML models in the following section.

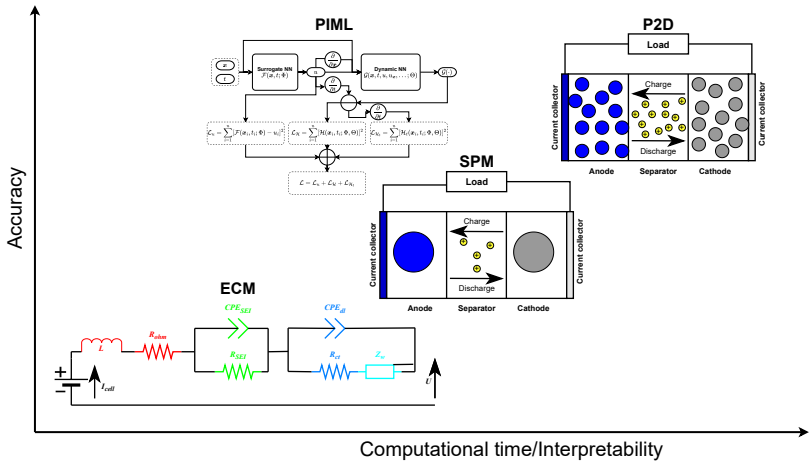

Figure 3.9: Accuracy versus computational time and interpretability for P2D, SPM, ECM, and PIML model [117].

Electrochemical Models

Battery degradation models depend on various underlying battery states (e.g., lithium concentration), which need to be simulated using an additional battery model during aging. One of the commonly used battery models for degradation simulation is the P2D model (also called the DFN model) based on porous electrode theory [83]. Specifically, the P2D model simulates lithium transport and diffusion in two dimensions, i.e., inside a spherical particle and along the thickness of a cell, which allows a gradient inside the particle depending on solid diffusion and a concentration gradient along the thickness of an electrode depending on electrolyte transport, respectively. However, the P2D model requires a large amount of computational effort to solve due to algebraic constraints.

By simulating only one particle in each electrode, the thickness dimension is removed from the P2D model. As a result, the SPM is obtained as the simplest electrochemical model that captures the average degradation of a cell [118] [119] [120]. Specifically, only solid state diffusion transport and spatially uniform kinetics are considered in the SPM. Although the validity range of the SPM may vary depending on the physico-chemical property of the cell (e.g., porosity and electrolyte conductivity), it is commonly accepted in the literature that the SPM is generally valid at currents below 1C [121] [122]. Therefore, the SPM may not be not valid for applications such as fast charging. Moreover, inhomogeneities and other local effects cannot be simulated either using the SPM model [49].

Physics-Based Degradation Models

SEI Growth Models

One of the most important degradation mechanisms at the anodes of lithium-ion batteries is SEI growth (see Subsection 2.3). In a reaction with lithium ions and electrons, electrolyte salts and solvents (see Subsection 2.1) are reduced at a potential that is higher than the intercalation potential of lithium ions. The resulting reaction products deposit on the graphite surface to form the SEI layer [123]. The SEI growth contributes to battery degradation in two ways, i.e., loss of lithium inventory and loss of active material of the negative electrode (see Subsection 2.3). Generally, physics-based SEI growth models can be divided into four categories, i.e., solvent diffusion-limited growth [85] [124] [125], reaction-limited growth [50] [120] [126], electron migration-limited growth [85] [125], and interstitial diffusion-limited growth [85].

Lithium Plating Models

Another degradation mechanism that occurs at the anode is lithium plating (see Subsection 2.3). Lithium plating takes place when lithium ions from the electrolyte form metallic lithium on the graphite surface instead of intercalating into it. Furthermore, lithium plating can occur with various degrees of reversibility within a cycle, which is defined as the ratio of lithium that is plated during charge and subsequently stripped to the electrolyte during discharge [57] [58]. The lithium plating contributes to battery degradation in two ways, i.e., loss of lithium inventory and loss of active material of the

negative electrode (see Fig. 2.4). Generally, standard Bulter-Volmer or Tafel kinetics are used in modeling the lithium plating/stripping process [48] [50] [87] [88] [127] [128] [129].

Particle Cracking Models

One degradation mechanism that occurs at both electrodes is particle cracking. Upon intercalation of lithium ions, the majority of electrode materials undergo expansion, followed by contraction upon deintercalation. The cyclic expansion and contraction of volume induce alternating stresses within the electrodes, resulting in particle cracking and crack propagation (see Section 2.3). The particle cracking contributes to battery degradation in two ways, i.e., loss of lithium inventory via accelerated SEI growth and loss of active material (see Fig. 2.5). Several particle cracking models have been proposed at the particle level [89] [90], and incorporated into a cell model [130].

Loss of Active Material Models

The loss of active material at both electrodes can be caused by various degradation mechanisms, such as transition metal dissolution, particle cracking, binder decomposition, loss of electric contact, etc (see Fig. 2.3). Loss of active material models that are based on different degradation mechanisms have been proposed in the literature. Generally, they can be divided into two categories, i.e., stress-induced loss of active material models [48] [90] and reaction-induced loss of active material models [91].

Physics-Informed Machine Learning

Machine learning models have demonstrated outstanding performance in various battery applications. However, they generally require large amounts of high-quality datasets for training, which are expensive to acquire in the lab and the field. Moreover, many ML models, particularly deep learning models, lack sufficient physical interpretability and struggle to generalize beyond the specific scenarios presented in the training data. In this regard, PIML addresses the challenges mentioned above by enforcing prior knowledge (or biases) from an empirical, physical, or mathematical understanding of the system into neural networks or other kernel-based models, such as Gaussian

processes [116]. Currently, three approaches can be employed separately or in tandem to enforce physics into ML models,

- Observational biases: Given sufficient data that embody the underlying physics, observational biases are conceptually the simplest mode of introducing biases in ML models during the training process. Examples include the deep operator network [131] and Fourier neural operator [132]. However, large amounts of high-quality data are typically required to reinforce these biases, and the acquisition cost could be formidable as observational data may be generated via expensive experiments or high-fidelity physics-based models.
- Inductive biases: Prior knowledge is incorporated into an ML model by crafting specialized architectures, such that predictions are strictly constrained by physics. Examples include convolutional neural networks [133], graph neural networks [134], and Gaussian processes [135]. However, inductive biases are limited to tasks that are characterized by relatively simple physics and challenging to implement in more complex tasks.
- Learning biases: Learning biases can be introduced into ML models by crafting loss functions, such that ML models simultaneously fit the observed data and yield predictions that are approximately constrained by physics. Although the underlying physics can only be approximately satisfied using such soft penalty constraints, there are also more flexibilities to enforce a wide range of physic-based biases into ML models. Examples include the deep Galerkin method [136], physics-informed neural networks (PINNs) [137], and model-integrated neural networks (MINNs) [138].

3.3 Scenario-Aware Machine Learning Pipeline

Advanced ML and PIML models have been developed to characterize battery degradation behaviors in various applications spanning battery design, manufacturing, usage, and repurposing stages [139]. To automate the process of selecting the best feature engineering method for developing the best model for a cell technology in a chosen scenario, a machine learning pipeline is introduced in Ref. [76], and extended here. As illustrated in Fig. 3.10,

the raw battery data (see Section 3.1) is first preprocessed and analyzed before stored in the database; Secondly, the modeler selects the cell technology (nominal capacity, chemistry, form factor, etc.) and the usage scenario (identical, protocol, or dynamic cycling); Thirdly, with the retrieved metadata, batteries are classified into different groups based on a desired criterion in the selected scenario (observed battery lifetime, nominal charging time, stress factors, etc.); Fourthly, the modeler selects the best feature engineering method (cycle-based, histogram-based, etc.) that extracts input features from time-series usage data at multiple sampling rates; Fifthly, the stratified random sampling method is used to split the input-output pairs, typically with 80% in the training set, and 20% in the test set. Moreover, equal ratios of batteries that belong to different groups are kept in the training and test set at each split; Sixthly, a wide range of ML and PIML models (see Section 3.2) are selected and their (hyper-)parameter values are optimized using the training set; Lastly, the performance of optimized ML and PIML models are evaluated on the test set, and the best model developed using the best feature engineering method at the optimal sampling rate is selected for the cell technology in the chosen scenario. Furthermore, the best ML or PIML model can be interpreted using techniques, such as permutation importance and partial dependence plot to rank feature importance and quantify the marginal effect of each feature on battery degradation behaviors.

The scenario-aware pipeline was initially introduced to develop ML and PIML models that characterize battery degradation behaviors in various applications. Furthermore, this pipeline can be easily adapted to develop the empirical or semi-empirical degradation models described in Section 3.2. However, physics-based models are known for poor identifiability and high conceptual complexity, and therefore, their parameterization is beyond the scope of this pipeline.

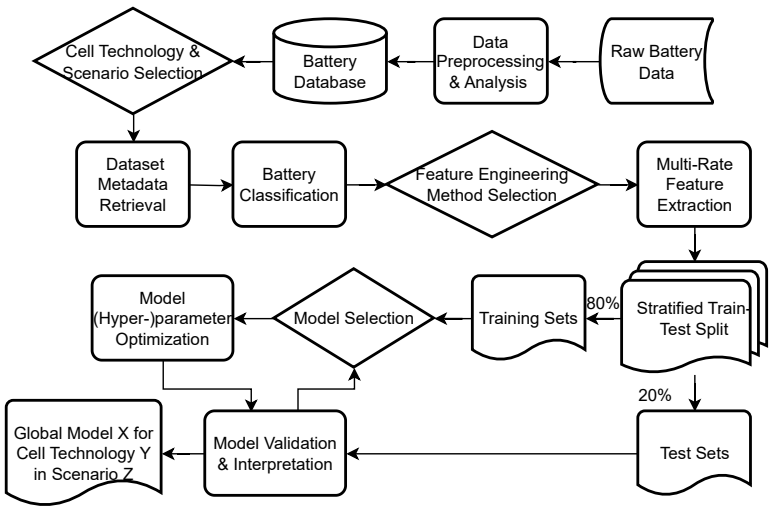

Figure 3.10: The scenario-aware machine learning pipeline.

CHAPTER 4

State-of-the-Art

In this chapter, four research problems addressed in this thesis will be described, and existing solution methods for each problem will be reviewed.

4.1 Battery Lifetime Prediction

Predicting the lifetime of a battery is of significant techno-economic importance for various applications at all stages of a battery's life [76] [139]. Applications that need battery lifetime prediction include fast-charging protocol optimization [61] and second-life repurposing [140]. Given the operating conditions, the goal of battery lifetime prediction is to determine the time or the number of (equivalent full) cycles until the battery reaches a predefined end-of-life (EoL) threshold. In the literature, the 70-80% of initial nominal capacity is commonly used as the EoL threshold. However, this EoL threshold solely focuses on capacity fade and neglects application specifications (e.g., driving range, charging time) and other battery characteristics (e.g., internal resistance/impedance). Therefore, EoL thresholds based on application specifications and other battery characteristics could be better definitions for batteries in first-life or second-life applications [141]. This section will review

lifetime prediction methods using lab data, discuss the challenges of lifetime prediction methods using field data, and at the second-life repurposing stage.

Battery Lifetime Prediction in the Lab

Historically, battery lifetime prediction has been restricted to using relatively small lab data under well-controlled operating conditions. Moreover, the EoL threshold is commonly based on relative capacity or relative resistance. Given identical cycling or similar protocol cycling conditions, predicting battery lifetime based on these fixed EoL thresholds is arguably acceptable in the lab. The battery models in lifetime prediction methods using lab data can be roughly divided into four categories, i.e.,

- Physics-based models: The electrochemical models may be coupled with multiple mechanical or chemical degradation models that capture underlying degradation mechanisms, such as the SEI growth [49] [85], lithium plating [49] [50] [129] [142], and particle cracking [49] [89] [90]. After model parameterization and validation with experimental data of a specific cell, these models could forecast the future battery states under certain operating conditions [143] [144]. Then the battery lifetime is predicted when the forecasted battery states reach a predefined EoL threshold.
- (Semi)-empirical models: After parameterizing (semi-)empirical models with experimental data of a specific cell, they are incorporated into a recursive Bayesian filter framework, such as a particle filter [53] [54] [145]. The model parameters are then recursively updated with onboard measured data. Lastly, the battery lifetime is predicted by identifying the point at which the predicted battery states reach a predefined EoL threshold.
- Machine learning models: Different from the aforementioned explicit battery models that capture the battery degradation process in the first place, some studies use machine learning models to learn a mapping function directly from input features, extracted from early degradation data to the battery lifetime, given a training set of input-output pairs [66] [146] [147]. In some other studies, the degradation process is firstly divided into a fixed number of time intervals, and then a mapping function is learned from input features extracted from usage patterns (e.g.,

the time spent within certain voltage, current, and temperature ranges) to battery state changes in the corresponding time intervals [110] [148]. In this way, the whole future battery state trajectory can be forecasted, and the battery lifetime is then predicted as the time when the forecasted state reaches a predefined EoL threshold.

Battery Lifetime Prediction in the Field

In contrast to high-quality lab data under well-controlled operating conditions, battery lifetime prediction using field data that contains realistic battery usage profiles in first-life in-vehicle applications and second-life stationary applications faces several challenges:

- In first-life in-vehicle applications, the reduction of battery capacity can be translated into the reduction of maximum driving distance, and therefore the EoL threshold is commonly based on relative capacity. However, this definition does consider application specifications. The state of function (SoF) that considers both battery characteristics and application specifications allows for a better definition of EoL threshold, i.e., 0% SoF in first-life or second-life applications [149].

- The field data is expected to be noisy due to highly varying battery usage profiles and fluctuating environmental conditions, sometimes missing due to long-time parking, and even corrupted due to faulty hardware or software. Additionally, unlike lab data, which is usually measured at the cell level, field data is measured at multi-levels, and therefore contains heterogeneity information within a module or a pack. It is therefore challenging for a pre-estimated model using lab data at the cell level to make accurate lifetime predictions using field data at multi-levels.

- To track the evolution of cell degradation throughout its life in the lab, regular reference performance tests (RPTs) are periodically conducted, in which three parameters are typically measured, i.e., capacity, internal resistance/impedance, and OCV (see Section 2.2). However, the aforementioned "ground truth" is lacking in the field, which is required to validate lifetime prediction methods.

Battery Lifetime Prediction at Repurposing

At the repurposing stage, the lifetime prediction of a battery in its intended second-life applications faces two major issues:

- Although the Global Battery Alliance has taken the initiative to enable battery data sharing using the battery passport [150], historical battery data that may contain information on its degradation pathway caused by first-life usage may still be unavailable or limited due to, for example, proprietary reason. Without additional battery characterization tests (see Section 2.2), battery lifetime prediction for its intended second-life application will be highly uncertain and application-dependent.
- The operating conditions will differ significantly between first-life in-vehicle and second-life stationary applications. Representative load profiles may first need to be extracted from different types of second-life applications. Then aging tests need to be conducted to characterize battery degradation in each second-life application in the lab. Notably, battery capacity knee must be considered in lifetime prediction at the repurposing stage as it can pose safety risks, particularly in second-life applications [151].

In summary, most studies have only focused on battery lifetime prediction based on fixed EoL thresholds using lab data, but very few studies have attempted to predict battery lifetime based on application-dependent EoL thresholds using lab or field data. Furthermore, battery lifetime prediction for repurposing used electric vehicle (EV) batteries to suitable second-life applications remains to be investigated.

4.2 Battery Capacity Knee Identification and Prediction

As a result of a complex interplay of various physical and chemical degradation mechanisms (see Section 2.3), the performance of lithium-ion battery cells degrades over their lives, for example, capacity fade and resistance/impedance rise. In some cases, sudden acceleration of capacity fade (so-called capacity knee) is observed to occur, which results in accelerated performance degradation and even safety issues of a cell [55]. Therefore, avoiding or at least

delaying the occurrence of the knee is essential to guarantee a long battery lifetime within safety constraints.

The IEEE Standard 485™-2020 defines the capacity knee as the transition when "the capacity slowly declines throughout most of the battery's life, but begins to decrease rapidly in the latter stages" [152]. However, this definition only qualitatively describes what a capacity knee is, and does not provide a method to identify the knee. In the literature, only a few studies have attempted to identify the knee on the capacity fade curve. They can be divided into two categories. One is intersection-based methods [148] [153] [154], and the other is learning-based methods [155] [156] [157]. In offline scenarios, the knee is identified given the complete capacity fade data of a cell with knee occurrence; while in online scenarios, the knee has to be identified on the fly during battery usage. The intersection-based methods use the intersection of two lines fitted to the beginning and the end of the capacity fade curve and can only be used offline. Specifically,

- The slope-changing ratio method: Prior to knee identification, an empirical model that characterizes the capacity fade curve with consideration of knee point occurrence is first proposed by Diao et al. [153]. After obtaining the fitted capacity fade curves, the knee is identified as the intersection of two tangent lines at two points, i.e., the points with minimum and maximum absolute slope, respectively. However, different degradation models may be required to fit different types of capacity fade curves.

- The Bacon-Watts method: By directly fitting the Bacon and Watts model [158] to the capacity fade data, the knee is identified as the intersection of two straight lines [154]. The Bacon-Watts method is simple and robust against noise without superimposing a degradation model, but may not be applicable to all types of capacity fade curves.

- The bisector method: The bisector method, proposed by Greenbank and Howey [148], first fits the early and late life capacity fade gradients using linear regression. Then the knee is identified as the intersection of an angle bisector of two gradients and the capacity fade curve. However, the bisector method is sensitive to the selection of early and late life capacity fade data, which may not be applicable to all types of capacity fade curves.

The learning-based methods use machine learning models to predict the knee point given specific features as inputs. Specifically,

- The quantile regression method: The quantile regression method, proposed by Zhang et al. [155], first fits a strip-shaped safety zone from experimental data (the height of the second IC peak), and the knee can be identified online as the last cycle of four consecutive cycles beyond the safety zone. Although the quantile regression method works with incoming data streams, the identified knees vary with the amount of available data online.

- The convolutional neural networks: The convolutional neural networks model, proposed by Sohn et al. [156], predicts the number of cycles to the knee point given input features extracted from time-series usage data. However, their method requires knee labeling beforehand using the Bacon-Watts model.

- The transformer-based deep learning model: The transformer-based deep learning model, proposed by Costa et al. [157], predicts whether or not a knee will occur within a window size of 800 cycles. Moreover, the model can also provide degradation diagnosis through quantifying degradation modes. However, it also requires knee labeling beforehand using a separate strategy.

In summary, intersection-based methods may fail as their effectiveness depends on the shape of the capacity fade curve, which can be linear, sublinear, superlinear, or a combination of the three [56]. Moreover, they cannot be used for online identification or prediction as they need more or less the complete fade curve. In contrast, learning-based methods can be used for online identification and prediction, but they usually require large amounts of labeled data for model offline training prior to their online deployment.

4.3 Battery Degradation Diagnosis

The goal of battery cell degradation diagnosis is to identify and quantify degradation modes inside a battery. Generally, diagnostic methods can be divided into three categories, i.e., post-mortem analysis, model-based analysis, and curve-based analysis [159]. The post-mortem analysis is a destructive

method that disassembles aged cells in a controlled environment, while the other two are non-invasive methods utilizing various sensing techniques, such as voltage, current, temperature, acoustic, strain, fiber-optic, etc.

Post-Mortem Analysis

Post-mortem analysis involves safely disassembling aged battery cells in a well-controlled clean environment and then carefully examining each of their components through material analysis, in order to identify and then quantify dominant degradation mechanisms [160] [161] [162]. From the physicochemical aspect, the post-mortem analysis can be further divided into three subcategories, i.e.,

- Morphology analysis: The morphology analysis is to examine the morphology of the electrode surface. Depending on different resolution requirements, optical microscopy [163], scanning electron microscopy [164], and transmission electron microscopy [165] are commonly used in morphology analysis.
- Composition analysis: The composition analysis is to examine the element composition of active materials and their concentration distribution on the electrode surface and at different depths. Techniques such as energy dispersive X-ray spectroscopy [161], X-ray photoelectron spectroscopy [166], inductively coupled plasma-atomic emission spectroscopy [167] have been reported to be used in the composition analysis.
- Structure analysis: The structure analysis is to examine the crystal structure on the surface, for which X-ray diffraction is commonly used [165].

Model-Based Analysis

The model-based diagnostic methods mainly involve electrochemical models derived from first principles using porous electrode theory (e.g., the Doyle-Fuller-Newman model [83], single particle model [84]), the mechanistic model [34], and equivalent circuit models [100].

- Electrochemical models: Some of the electrochemical model parameters are important health indicators, which are closely related to the

degradation of lithium-ion battery cells [168] [169] [170]. Therefore, identifying these aging parameters in electrochemical models and then correlating them with underlying degradation mechanisms and modes would facilitate battery degradation diagnosis. Some aging parameters in electrochemical models that have been identified in the literature are the volume fraction of active material at the anode [171], solid electrolyte interphase (SEI) resistance [171], the resistance of deposit layer [171], the electrolyte diffusion coefficient [171], positive and negative solid phase diffusion coefficient [168], positive and negative electrochemical reaction rate constant [168], the cathode particle surface area [169], stoichiometry limits [169], and porosities of the cathode, separator, and anode [169].

- The mechanistic model: A mechanistic model that can simulate various "what-if" scenarios of battery degradation modes and enable online battery degradation diagnosis via incremental capacity (IC) and differential voltage (DV) curves was proposed by Dubarry et al. [34]. The model can simulate individual electrode behavior with two model parameters, i.e., the loading ratio between the negative and positive electrode, and the initial irreversible capacity loss of the negative electrode that compensates the SEI formation.

- Equivalent circuit models: The experimental data obtained from electrochemical impedance spectroscopy (EIS) tests contains rich information about cell degradation caused by internal resistance/impedance (see Subsubsection 2.2) and can therefore be used to identify cell degradation mechanisms [32] [33]. Typically, the impedance spectrum of a cell is represented by a Nyquist plot, which is often modeled by an equivalent circuit model (ECM). As a commonly-used model, the adapted Randles-equivalent circuit model (AR-ECM) is illustrated in Fig. 4.1, in which changes of four resistances (ohmic R_{ohm}, SEI R_{SEI}, charge-transfer R_{ct}, and Warburg R_w) are tracked to identify and quantify degradation mechanisms, i.e., ohmic resistance increase (ORI), loss of lithium inventory (LLI), and loss of active material (LAM) [32].

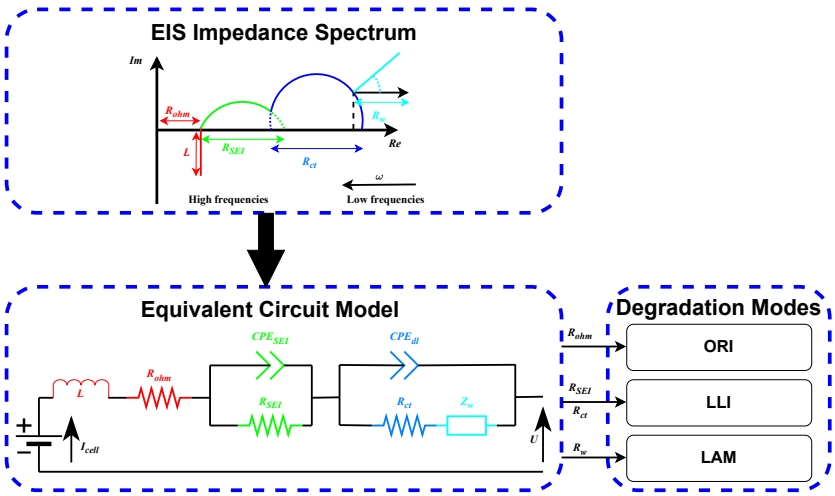

Figure 4.1: Using EIS impedance spectrum and ECM to identify degradation mechanisms [32].

Curve-Based Analysis

As it is illustrated in Fig. 4.2, most physics-based models generally capture the most dominant degradation mechanisms at the micro-scale [89] or even nano-scale [172]. However, previous studies have illustrated that meso-scale and macro-scale inhomogeneities in the structure of the electrodes caused by cell manufacture can have a significant impact on safety (e.g., thermal runaway [173]) and cell degradation in the long term (e.g., capacity knee occurrence [47]), which may not be captured by bottom-up physics-based models.

Curve-based analysis methods that utilize measurements from cell characterization tests (see Section 2.2) provide an alternative solution to cell degradation diagnosis. Examples of utilizing different measurements from cell characterization tests are:

- EIS impedance spectrum [33].
- Discharge voltage curve [66].
- Pseudo open circuit voltage (OCV) [46].

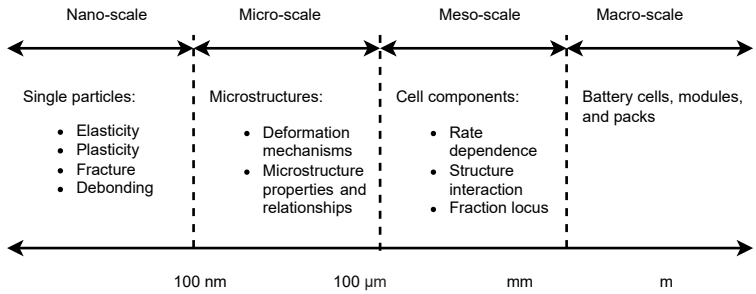

Figure 4.2: Mechanical properties of lithium-ion batteries at different length scales [174].

- Derivatives of OCV or cell capacity, such as incremental capacity analysis (ICA) [21] and differential voltage analysis (DVA) [22].

In summary, as an invasive method, the post-mortem analysis is infeasible for online battery degradation diagnosis but can provide the "ground truth" of battery degradation. In contrast, the model-based and curve-based analyses have the potential to achieve effective and non-invasive online battery degradation diagnosis.

4.4 Energy Management in Grid-Connected Microgrids

There are many stationary applications where used or second-life EV batteries can be repurposed. These stationary applications span over residential, commercial & industrial, and utility scenarios [175]. In the literature, most studies focus on grid-connected microgrids consisting of renewable energy sources (RESs) and battery energy storage systems (BESSs). However, safe and optimal usage of second-life BESSs in grid-connected microgrids still faces challenges, particularly concerning decision-making under different types of uncertainty. Specifically, the uncertainty mainly arises from forecasts of load demand, RESs production, electricity prices, and battery degradation. Various control strategies with different objectives have been proposed for en-

ergy management in grid-connected microgrids. These control strategies can be divided into three categories, i.e.,

- Rule-based strategies: There are two commonly used rule-based strategies, i.e., 1) maximizing self-consumption (MSC) is to maximize the use of RESs production for load demand and battery charge; 2) time-of-use (ToU) is to maximize the economic benefit with the difference between peak and valley electricity prices. Both rule-based strategies are developed based on the difference between RESs production and load demand, and the electricity prices [176]. The rule-based strategies are easy to implement but less adaptive to different types of uncertainty.

- Model predictive control (MPC): MPC finds an (implicit) feedback policy at each time instant by solving an optimal control problem in a receding-horizon fashion [177]. Different objectives can be taken into account, for example, stability and constraints satisfaction using tracking MPC, and closed-loop performance using economic MPC. Moreover, the uncertainties associated with fluctuations in RESs production, load demand, and electricity prices, can be addressed via robust or stochastic MPC [178]. However, MPC has two drawbacks: 1) For computational reasons, simple models are preferred in the MPC scheme. As a result, the MPC-based solution is optimal for the given model, but suboptimal for the real system with uncertainties; 2) It is difficult to consider long-term objectives and constraints due to the finite-horizon formulation of MPC.

- Reinforcement learning (RL): RL learns a policy that maps states to actions by directly interacting with the environment or indirectly from collected historical data [179]. The effects of uncertainties in the system can be reduced with sufficient exploration or good use of data [180]. However, RL tends to suffer from two difficulties: 1) A large amount of data is required for model-free RL to learn a satisfactory policy; 2) RL theory is immature to handle system constraints and evaluate closed-loop stability.

CHAPTER 5

Summary of included papers

This chapter provides a summary of the included papers.

5.1 Paper A

Huang Zhang, Yang Su, Faisal Altaf, Torsten Wik, and Sébastien Gros
Interpretable Battery Cycle Life Range Prediction Using Early Cell Degradation Data
Published in IEEE Transactions on Transportation Electrification, vol. 9, no. 2, pp. 2669–2682, Dec. 2022.
 DOI: 10.1109/TTE.2022.3226683 .

Battery lifetime prediction using early degradation data has many applications throughout the battery product life cycle. To address this research problem, the quantile regression forests (QRF) model is introduced in this paper to provide cycle life range prediction with uncertainty quantified as the width of the prediction interval, in addition to point predictions with high accuracy. The prediction performance of the QRF model is demonstrated on a publicly available battery dataset under realistic fast-charging protocols.

Using two model-agnostic interpretation techniques, the two most important input features are identified and their effect on predicted battery cycle life is quantitatively investigated. An important advantage of this method compared to others is that no assumptions on the statistical distribution have to be made, which otherwise easily corrupts uncertainty estimates..

Huang Zhang contributed with Conceptualization, Methodology, Software, Data curation, Validation, Formal analysis, Investigation, and Writing – original draft. **Yang Su** contributed with Resources, Methodology, and Writing – review & editing. **Faisal Altaf** contributed with Resources, Writing – review & editing, Supervision, Project administration, and Funding acquisition. **Torsten Wik** contributed with Resources, Writing – review & editing, Supervision, and Funding acquisition. **Sébastien Gros** contributed with Resources, Writing – review & editing, Supervision, and Funding acquisition.

5.2 Paper B

Huang Zhang, Faisal Altaf, Torsten Wik, and Sébastien Gros
Comparative Analysis of Battery Cycle Life Early Prediction Using Machine Learning Pipeline
Published in proceedings of the 22nd IFAC World Congress,
vol. 56, no. 2, pp. 3757–3763, Jul. 2023.
 DOI: 10.1016/j.ifacol.2023.10.1545 .

Lithium-ion battery system is one of the most critical but expensive components for both electric vehicles and stationary energy storage applications. In this paper, to produce the best model for both battery cycle life point prediction and range prediction (i.e., confidence intervals or prediction intervals), a pipeline-based approach is proposed, in which a full 33-feature set is generated manually based on battery degradation knowledge, and then used to learn the best model among five machine learning (ML) models that have been reported in the battery lifetime prediction literature, and two quantile regression models for battery cycle life prediction. The calibration and sharpness property of battery cycle life range prediction is properly evaluated by their coverage probability and width respectively. The experimental results show that the gradient boosting regression tree model provides the best point prediction performance, while the quantile regression forest model provides

the best range prediction performance with both full 33-feature set and the MIT 6-feature set.

Huang Zhang contributed with Conceptualization, Methodology, Software, Data curation, Validation, Formal analysis, Investigation, and Writing – original draft. **Faisal Altaf** contributed with Resources, Writing – review & editing, Supervision, Project administration, and Funding acquisition. **Torsten Wik** contributed with Resources, Writing – review & editing, Supervision, and Funding acquisition. **Sébastien Gros** contributed with Resources, Writing – review & editing, Supervision, and Funding acquisition.

5.3 Paper C

Huang Zhang, Faisal Altaf, and Torsten Wik
Scenario-Aware Machine Learning Pipeline for Battery Lifetime Prediction
Published in proceedings of 2024 European Control Conference,
pp. 212–217, Jul. 2024.
 DOI: 10.23919/ECC64448.2024.10591037 .

Advanced machine learning (ML) models have been developed for battery lifetime prediction in different use cases at all stages of a battery's life. As the first step to enable the transferability of ML models for battery lifetime prediction across multiple use cases, a scenario-aware machine learning pipeline is proposed, in which two feature engineering methods that have been able to generate input features with outstanding predictive power are used to learn the best ML model for battery lifetime prediction in a chosen usage scenario. The experimental results show that the histogram-based feature engineering method is able to generate input features with predictive power generalized across two usage scenarios (i.e., identical cycling and protocol cycling). Thus, to enable transferability of ML models for battery lifetime prediction across different scenarios, and even battery chemistries, this histogram-based feature engineering method will be further investigated together with online fine-tuning strategies.

Huang Zhang contributed with Conceptualization, Methodology, Software, Data curation, Validation, Formal analysis, Investigation, and Writing – original draft. **Faisal Altaf** contributed with Resources, Writing – review & editing, Supervision, Project administration, and Funding acquisition.

Torsten Wik contributed with Resources, Writing – review & editing, Supervision, and Funding acquisition.

5.4 Paper D

Huang Zhang, Faisal Altaf, and Torsten Wik
Battery Capacity Knee-Onset Identification and Early Prediction Using Degradation Curvature
Published in Journal of Power Sources,
vol. 608, pp. 234619, Jul. 2024.
 DOI: 10.1016/j.jpowsour.2024.234619 .

Abrupt capacity fade can have a significant impact on performance and safety in battery applications. To address concerns arising from possible knee occurrence, this work aims for a better understanding of their cause by introducing a new definition of capacity knees and their onset. A curvature-based identification of a knee and its onset is proposed, which relies on the discovery of a distinctly fluctuating behavior in the transition between an initial and a final stable acceleration of the degradation. The method is validated on experimental degradation data of two different battery chemistries, synthetic degradation data, and is also benchmarked to the state-of-the-art knee identification method in the literature. The results demonstrate that our proposed method could successfully identify capacity knees when the state-of-the-art knee identification method failed. Furthermore, a significantly strong correlation is found between knee and end of life (EoL) and almost equally strong between knee onset and EoL. As the method does not require the full capacity fade curve, this opens up online knee-onset identification as well as knee and EoL prediction.

Huang Zhang contributed with Conceptualization, Methodology, Software, Data curation, Validation, Formal analysis, Investigation, and Writing – original draft. **Faisal Altaf** contributed with Resources, Writing – review & editing, Supervision, Project administration, and Funding acquisition. **Torsten Wik** contributed with Resources, Writing – review & editing, Supervision, and Funding acquisition.

5.5 Paper E

Huang Zhang, Xixi Liu, Faisal Altaf, and Torsten Wik
A Transferable Physics-Informed Framework for Battery Degradation Diagnosis, Knee-Onset Detection and Knee Prediction
Submitted .

The techno-economic and safety concerns of battery capacity knee occurrence call for developing online knee detection and prediction methods as an advanced battery management system (BMS) function. To address this, a transferable physics-informed framework that consists of a histogram-based feature engineering method, a hybrid physics-informed model, and a fine-tuning strategy, is proposed for online battery degradation diagnosis and knee-onset detection. The hybrid model is first developed and evaluated using a scenario-aware pipeline in protocol cycling scenarios and then fine-tuned to create a local model deployed in a dynamic cycling scenario. A 2D histogram-based feature set is found to be the best choice in both source and target scenarios. The fine-tuning strategy is proven to be effective in improving battery degradation mode estimation and degradation phase detection performance in the target scenario. Again, a strong linear correlation was found between the identified knee-onset and knee points. As a result, advanced BMS functions, such as online degradation diagnosis and prognosis, online knee-onset detection and knee prediction, aging-aware battery classification, and second-life repurposing, can be enabled through a battery performance digital twin in the cloud.

Huang Zhang contributed with Conceptualization, Methodology, Software, Data curation, Validation, Formal analysis, Investigation, Writing – original draft, Project administration, and Funding acquisition. **Xixi Liu** contributed with Resources, and Writing – review & editing. **Faisal Altaf** contributed with Resources, Writing – review & editing, Supervision, and Funding acquisition. **Torsten Wik** contributed with Resources, Writing – review & editing, Supervision, and Funding acquisition.

5.6 Paper F

Huang Zhang, Faisal Altaf, and Torsten Wik
Comparative Study of Aging-Aware Control Strategies for Grid-Connected

Photovoltaic Battery Systems
Published in proceedings of the 63rd IEEE Conference on Decision and Control
pp. 3501–3507, Dec. 2024.
 DOI: 10.1109/CDC56724.2024.10886263 .

Various strategies with different objectives have been proposed to control grid-connected photovoltaic (PV) battery systems where electric vehicle (EV) batteries can be used as stationary energy storage. As the first attempt to enable aging-aware decision-making under various uncertainties, an economically motivated stage cost function is proposed to account for both the grid and the battery degradation cost. Historical operational data and "fixed" forecasted electricity price data are utilized to improve the economic performance of an implicit (or time-varying) optimal policy. Simulation results show that an implicit optimal policy achieved better economic performance (i.e., lowest grid and battery degradation cost) with smaller fluctuation amplitudes than an explicit one. Thus, to improve the aging-aware decision-making under uncertainties for EV batteries further, the implicit optimal policy will be further developed with consideration of other forecasts.

Huang Zhang contributed with Conceptualization, Methodology, Software, Data curation, Validation, Formal analysis, Investigation, Writing – original draft, Project administration, and Funding acquisition. **Faisal Altaf** contributed with Resources, Writing – review & editing, Supervision, and Funding acquisition. **Torsten Wik** contributed with Resources, Writing – review & editing, Supervision, and Funding acquisition.

5.7 Paper G

Huang Zhang, Xixi Liu, Faisal Altaf, and Torsten Wik
A Practitioner's Guide to Automatic Kernel Search for Gaussian Processes in Battery Applications
Submitted to the 64th IEEE Conference on Decision and Control .

Gaussian process (GP) models have been used in a wide range of battery applications, in which different kernels were manually selected with considerable expertise. However, to capture complex relationships in the ever-growing amount of real-world data, selecting a suitable kernel for the GP model in

battery applications is increasingly challenging. In this work, we first review existing GP kernels used in battery applications and then extend an automatic kernel search method with a new base kernel and model selection criteria. The GP models with composite kernels outperform the baseline kernel in two numerical examples of battery applications, i.e., battery capacity estimation and residual load prediction. Particularly, the results indicate that the Bayesian Information Criterion may be the best model selection criterion as it achieves a good trade-off between kernel performance and computational complexity. This work should, therefore, be of value to practitioners wishing to automate their kernel search process in battery applications.

Huang Zhang contributed with Conceptualization, Methodology, Software, Data curation, Validation, Formal analysis, Investigation, Writing – original draft, Project administration, and Funding acquisition. **Xixi Liu** contributed with Resources, Methodology, and Writing – review & editing. **Faisal Altaf** contributed with Resources, Writing – review & editing, Supervision, and Funding acquisition. **Torsten Wik** contributed with Resources, Writing – review & editing, Supervision, and Funding acquisition.

CHAPTER 6

Concluding Remarks and Future Work

Second-life applications of electric vehicle (EV) batteries will arguably have economic, technical, and environmental benefits. However, for safe and optimal usage of EV batteries in second-life applications, important factors, such as battery lifetime, cell-to-cell variations, second-life application specifications, cost and benefits of second-life battery energy storage systems (BESSs) in various applications, and relevant market forecasts, must be considered in the sequential decision-making process. In this thesis, our main goal is to enable successful market adoption of second-life BESSs based on new and used EV batteries. To achieve this, we proposed aging-aware classification in first-life applications and optimal usage in second-life applications for EV batteries. Specifically, four research problems have been addressed in this thesis, i.e., 1) battery lifetime early prediction; 2) battery capacity knee identification and knee-onset early prediction; 3) battery degradation mode estimation and phase detection; 4) energy management in grid-connected microgrids.

The key results and contributions are summarized as follows: 1) To provide battery lifetime prediction using early degradation data, the quantile regression forests (QRF) model was introduced for battery cycle life prediction with uncertainty quantified. Two model-agonistic interpretation techniques were

employed to identify the most important input feature and then quantify its effect on the predicted battery cycle life. Furthermore, a scenario-aware machine learning (ML) pipeline was proposed to automate the process of developing the best battery lifetime prediction model in a chosen scenario; 2) To identify knee and knee-onset points on the battery capacity fade curve, a curvature-based identification method was proposed. Even though the state-of-the-art method failed, this method could still identify capacity knees as it relies on the discovery of an oscillatory degradation phenomenon; 3) To enable online classification of EV batteries, a transfer learning-based physics-informed framework was proposed to first estimate battery degradation modes and then detect the degradation phase using aggregated time-series voltage data. Advanced battery management functions, such as online degradation diagnosis and second-life repurposing could also be enabled using the proposed framework in a battery digital twin; 4) To enable optimal usage of EV batteries in second-life applications, an economic stage cost function was proposed to account for both the grid and the battery degradation cost in grid-connected microgrids, and an automatic kernel search method was extended with a new base kernel and model selection criteria to construct the best composite kernel in Gaussian process (GP) regression models for battery capacity estimation and residual load prediction in grid-connected microgrids. The proposed cost function and kernel search method will be used in our future work.

Finally, some advances can be made in future work, i.e., 1) Instead of fixed end-of-life (EoL) thresholds, application-dependent EoL thresholds are better choices in battery lifetime prediction for first-life and second-life applications; 2) The oscillatory degradation phenomenon was found to be essential to the effectiveness of the proposed capacity knee identification method. It is, therefore, worth further investigating this oscillatory degradation phenomenon using synthetic and experimental datasets covering more knee pathways; 3) To maximize the overall value of EV batteries before eventually being recycled, the proposed cost function and kernel search method will be used to develop a techno-economic model with which EV batteries can be repurposed for second-life applications at a good time.

References

[1] International Energy Agency, "CO2 emissions in 2023," International Energy Agency (IEA), Tech. Rep., 2023.

[2] International Energy Agency, "World energy outlook 2023," International Energy Agency (IEA), Tech. Rep., 2023.

[3] International Energy Agency, "Global ev outlook 2024: Moving towards increased affordability," International Energy Agency (IEA), Tech. Rep., 2024.

[4] B. Faessler, "Stationary, second use battery energy storage systems and their applications: A research review," *Energies*, vol. 14, no. 8, p. 2335, 2021.

[5] A. A. Kebede, T. Kalogiannis, J. Van Mierlo, and M. Berecibar, "A comprehensive review of stationary energy storage devices for large scale renewable energy sources grid integration," *Renewable and Sustainable Energy Reviews*, vol. 159, p. 112 213, 2022.

[6] R. Reinhardt, I. Christodoulou, S. Gassó-Domingo, and B. A. García, "Towards sustainable business models for electric vehicle battery second use: A critical review," *Journal of environmental management*, vol. 245, pp. 432–446, 2019.

[7] A. Khowaja, M. D. Dean, and K. M. Kockelman, "Quantifying the emissions impact of repurposed electric vehicle battery packs in residential settings," *Journal of Energy Storage*, vol. 47, p. 103 628, 2022.

[8] J. Deng, C. Bae, A. Denlinger, and T. Miller, "Electric vehicles batteries: Requirements and challenges," *Joule*, vol. 4, no. 3, pp. 511–515, 2020.

[9] K. W. Beard, *Linden's handbook of batteries*. McGraw-Hill Education, 2019.

[10] G. E. Blomgren, "The development and future of lithium ion batteries," *Journal of The Electrochemical Society*, vol. 164, no. 1, A5019, 2016.

[11] R. Schmuch, R. Wagner, G. Hörpel, T. Placke, and M. Winter, "Performance and cost of materials for lithium-based rechargeable automotive batteries," *Nature Energy*, vol. 3, no. 4, pp. 267–278, 2018.

[12] G. Dang, M. Zhang, F. Min, *et al.*, "Lithium titanate battery system enables hybrid electric heavy-duty vehicles," *Journal of Energy Storage*, vol. 74, p. 109 313, 2023.

[13] R. Wang, W. Cui, F. Chu, and F. Wu, "Lithium metal anodes: Present and future," *Journal of Energy Chemistry*, vol. 48, pp. 145–159, 2020.

[14] J. S. Edge, S. O'Kane, R. Prosser, *et al.*, "Lithium ion battery degradation: What you need to know," *Physical Chemistry Chemical Physics*, vol. 23, no. 14, pp. 8200–8221, 2021.

[15] H.-J. Noh, S. Youn, C. S. Yoon, and Y.-K. Sun, "Comparison of the structural and electrochemical properties of layered li [nixcoymnz] o2 (x= 1/3, 0.5, 0.6, 0.7, 0.8 and 0.85) cathode material for lithium-ion batteries," *Journal of power sources*, vol. 233, pp. 121–130, 2013.

[16] Y.-K. Liu, C.-Z. Zhao, J. Du, X.-Q. Zhang, A.-B. Chen, and Q. Zhang, "Research progresses of liquid electrolytes in lithium-ion batteries," *Small*, vol. 19, no. 8, p. 2 205 315, 2023.

[17] Y. An, X. Han, Y. Liu, *et al.*, "Progress in solid polymer electrolytes for lithium-ion batteries and beyond," *Small*, vol. 18, no. 3, p. 2 103 617, 2022.

[18] N. Lingappan, W. Lee, S. Passerini, and M. Pecht, "A comprehensive review of separator membranes in lithium-ion batteries," *Renewable and Sustainable Energy Reviews*, vol. 187, p. 113 726, 2023.

[19] A. Barai, K. Uddin, M. Dubarry, *et al.*, "A comparison of methodologies for the non-invasive characterisation of commercial li-ion cells," *Progress in Energy and Combustion Science*, vol. 72, pp. 1–31, 2019.

[20] J. Groot, *State-of-health estimation of li-ion batteries: Cycle life test methods*. Chalmers Tekniska Högskola (Sweden), 2012.

[21] M. Dubarry, V. Svoboda, R. Hwu, and B. Y. Liaw, "Incremental capacity analysis and close-to-equilibrium ocv measurements to quantify capacity fade in commercial rechargeable lithium batteries," *Electrochemical and solid-state letters*, vol. 9, no. 10, A454, 2006.

[22] I. Bloom, A. N. Jansen, D. P. Abraham, *et al.*, "Differential voltage analyses of high-power, lithium-ion cells: 1. technique and application," *Journal of Power Sources*, vol. 139, no. 1-2, pp. 295–303, 2005.

[23] K. Uddin, L. Somerville, A. Barai, *et al.*, "The impact of high-frequency-high-current perturbations on film formation at the negative electrode-electrolyte interface," *Electrochimica Acta*, vol. 233, pp. 1–12, 2017.

[24] U. S. A. B. Consortium *et al.*, "Electric vehicle battery test procedures manual," *USABC, Jan*, 1996.

[25] F. Sun, R. Xiong, H. He, W. Li, and J. E. E. Aussems, "Model-based dynamic multi-parameter method for peak power estimation of lithium–ion batteries," *Applied Energy*, vol. 96, pp. 378–386, 2012.

[26] X. Lin, Y. Tang, J. Ren, and Y. Wei, "State of charge estimation with the adaptive unscented kalman filter based on an accurate equivalent circuit model," *Journal of Energy Storage*, vol. 41, p. 102 840, 2021.

[27] Y. Ye, Y. Shi, N. Cai, J. Lee, and X. He, "Electro-thermal modeling and experimental validation for lithium ion battery," *Journal of Power Sources*, vol. 199, pp. 227–238, 2012.

[28] J. Wang, J. Purewal, P. Liu, *et al.*, "Degradation of lithium ion batteries employing graphite negatives and nickel–cobalt–manganese oxide+ spinel manganese oxide positives: Part 1, aging mechanisms and life estimation," *Journal of Power Sources*, vol. 269, pp. 937–948, 2014.

[29] Z. Deng, Z. Zhang, Y. Lai, J. Liu, J. Li, and Y. Liu, "Electrochemical impedance spectroscopy study of a lithium/sulfur battery: Modeling and analysis of capacity fading," *Journal of The Electrochemical Society*, vol. 160, no. 4, A553, 2013.

[30] H. Beelen, L. Raijmakers, M. Donkers, P. Notten, and H. Bergveld, "A comparison and accuracy analysis of impedance-based temperature estimation methods for li-ion batteries," *Applied Energy*, vol. 175, pp. 128–140, 2016.

[31] S. Alavi, C. Birkl, and D. Howey, "Time-domain fitting of battery electrochemical impedance models," *Journal of Power Sources*, vol. 288, pp. 345–352, 2015.

[32] C. Pastor-Fernández, W. D. Widanage, J. Marco, M.-Á. Gama-Valdez, and G. H. Chouchelamane, "Identification and quantification of ageing mechanisms in lithium-ion batteries using the EIS technique," in *2016 IEEE Transportation Electrification Conference and Expo (ITEC)*, IEEE, 2016, pp. 1–6.

[33] Y. Zhang, Q. Tang, Y. Zhang, J. Wang, U. Stimming, and A. A. Lee, "Identifying degradation patterns of lithium ion batteries from impedance spectroscopy using machine learning," *Nature communications*, vol. 11, no. 1, p. 1706, 2020.

[34] M. Dubarry, C. Truchot, and B. Y. Liaw, "Synthesize battery degradation modes via a diagnostic and prognostic model," *Journal of power sources*, vol. 219, pp. 204–216, 2012.

[35] C. R. Birkl, E. McTurk, M. Roberts, P. G. Bruce, and D. A. Howey, "A parametric open circuit voltage model for lithium ion batteries," *Journal of The Electrochemical Society*, vol. 162, no. 12, A2271, 2015.

[36] C. Truchot, M. Dubarry, and B. Y. Liaw, "State-of-charge estimation and uncertainty for lithium-ion battery strings," *Applied Energy*, vol. 119, pp. 218–227, 2014.

[37] W. Lee, "United states advanced battery consortium battery test manual for electric vehicles," Idaho National Laboratory, Tech. Rep., 2020.

[38] S. Lim, J.-H. Kim, Y. Yamada, *et al.*, "Improvement of rate capability by graphite foam anode for li secondary batteries," *Journal of Power Sources*, vol. 355, pp. 164–170, 2017.

[39] A. Barai, W. D. Widanage, J. Marco, A. McGordon, and P. Jennings, "A study of the open circuit voltage characterization technique and hysteresis assessment of lithium-ion cells," *Journal of Power Sources*, vol. 295, pp. 99–107, 2015.

[40] F.-A. LeBel, P. Messier, A. Sari, and J. P. F. Trovão, "Lithium-ion cell equivalent circuit model identification by galvanostatic intermittent titration technique," *Journal of Energy Storage*, vol. 54, p. 105 303, 2022.

[41] B. Rumberg, B. Epding, I. Stradtmann, and A. Kwade, "Identification of li ion battery cell aging mechanisms by half-cell and full-cell open-circuit-voltage characteristic analysis," *Journal of Energy Storage*, vol. 25, p. 100 890, 2019.

[42] M. Dubarry and B. Y. Liaw, "Identify capacity fading mechanism in a commercial lifepo4 cell," *Journal of power sources*, vol. 194, no. 1, pp. 541–549, 2009.

[43] M. García-Plaza, J. E.-G. Carrasco, A. Peña-Asensio, J. Alonso-Martínez, and S. A. Gómez, "Hysteresis effect influence on electrochemical battery modeling," *Electric Power Systems Research*, vol. 152, pp. 27–35, 2017.

[44] Y. Xing, W. He, M. Pecht, and K. L. Tsui, "State of charge estimation of lithium-ion batteries using the open-circuit voltage at various ambient temperatures," *Applied Energy*, vol. 113, pp. 106–115, 2014.

[45] J. Vetter, P. Novák, M. R. Wagner, *et al.*, "Ageing mechanisms in lithium-ion batteries," *Journal of power sources*, vol. 147, no. 1-2, pp. 269–281, 2005.

[46] C. R. Birkl, M. R. Roberts, E. McTurk, P. G. Bruce, and D. A. Howey, "Degradation diagnostics for lithium ion cells," *Journal of Power Sources*, vol. 341, pp. 373–386, 2017.

[47] T. C. Bach, S. F. Schuster, E. Fleder, *et al.*, "Nonlinear aging of cylindrical lithium-ion cells linked to heterogeneous compression," *Journal of Energy Storage*, vol. 5, pp. 212–223, 2016.

[48] S. E. O'Kane, W. Ai, G. Madabattula, *et al.*, "Lithium-ion battery degradation: How to model it," *Physical Chemistry Chemical Physics*, vol. 24, no. 13, pp. 7909–7922, 2022.

[49] J. M. Reniers, G. Mulder, and D. A. Howey, "Review and performance comparison of mechanical-chemical degradation models for lithium-ion batteries," *Journal of The Electrochemical Society*, vol. 166, no. 14, A3189–A3200, 2019.

[50] X.-G. Yang, Y. Leng, G. Zhang, S. Ge, and C.-Y. Wang, "Modeling of lithium plating induced aging of lithium-ion batteries: Transition from linear to nonlinear aging," *Journal of Power Sources*, vol. 360, pp. 28–40, 2017.

[51] X. Lin, J. Park, L. Liu, Y. Lee, A. Sastry, and W. Lu, "A comprehensive capacity fade model and analysis for li-ion batteries," *Journal of The Electrochemical Society*, vol. 160, no. 10, A1701, 2013.

[52] S. J. An, J. Li, C. Daniel, D. Mohanty, S. Nagpure, and D. L. Wood III, "The state of understanding of the lithium-ion-battery graphite solid electrolyte interphase (sei) and its relationship to formation cycling," *Carbon*, vol. 105, pp. 52–76, 2016.

[53] W. He, N. Williard, M. Osterman, and M. Pecht, "Prognostics of lithium-ion batteries based on dempster–shafer theory and the bayesian monte carlo method," *Journal of Power Sources*, vol. 196, no. 23, pp. 10 314–10 321, 2011.

[54] F. Yang, D. Wang, Y. Xing, and K.-L. Tsui, "Prognostics of li (nimnco) o2-based lithium-ion batteries using a novel battery degradation model," *Microelectronics Reliability*, vol. 70, pp. 70–78, 2017.

[55] E. Martinez-Laserna, E. Sarasketa-Zabala, I. V. Sarria, *et al.*, "Technical viability of battery second life: A study from the ageing perspective," *IEEE Transactions on Industry Applications*, vol. 54, no. 3, pp. 2703–2713, 2018.

[56] P. M. Attia, A. Bills, F. B. Planella, *et al.*, ""knees" in lithium-ion battery aging trajectories," *Journal of The Electrochemical Society*, vol. 169, no. 6, p. 060 517, 2022.

[57] M. Dubarry and D. Beck, "Big data training data for artificial intelligence-based li-ion diagnosis and prognosis," *Journal of Power Sources*, vol. 479, p. 228 806, 2020.

[58] X. Lin, K. Khosravinia, X. Hu, J. Li, and W. Lu, "Lithium plating mechanism, detection, and mitigation in lithium-ion batteries," *Progress in Energy and Combustion Science*, vol. 87, p. 100 953, 2021.

[59] X.-G. Yang and C.-Y. Wang, "Understanding the trilemma of fast charging, energy density and cycle life of lithium-ion batteries," *Journal of Power Sources*, vol. 402, pp. 489–498, 2018.

[60] E. Coron, S. Geniès, M. Cugnet, and P. Thivel, "Impact of lithium-ion cell condition on its second life viability," *Journal of The Electrochemical Society*, vol. 167, no. 11, p. 110 556, 2020.

[61] P. M. Attia, A. Grover, N. Jin, *et al.*, "Closed-loop optimization of fast-charging protocols for batteries with machine learning," *Nature*, vol. 578, no. 7795, pp. 397–402, 2020.

[62] M. Klett, P. Svens, C. Tengstedt, *et al.*, "Uneven film formation across depth of porous graphite electrodes in cycled commercial li-ion batteries," *The Journal of Physical Chemistry C*, vol. 119, no. 1, pp. 90–100, 2015.

[63] S. F. Schuster, T. Bach, E. Fleder, *et al.*, "Nonlinear aging characteristics of lithium-ion cells under different operational conditions," *Journal of Energy Storage*, vol. 1, pp. 44–53, 2015.

[64] E. Deichmann, L. Torres-Castro, J. Lamb, *et al.*, "Investigating the effects of lithium deposition on the abuse response of lithium-ion batteries," *Journal of The Electrochemical Society*, vol. 167, no. 9, p. 090 552, 2020.

[65] D. Anseán, M. Dubarry, A. Devie, *et al.*, "Operando lithium plating quantification and early detection of a commercial lifepo4 cell cycled under dynamic driving schedule," *Journal of Power Sources*, vol. 356, pp. 36–46, 2017.

[66] K. A. Severson, P. M. Attia, N. Jin, *et al.*, "Data-driven prediction of battery cycle life before capacity degradation," *Nature Energy*, vol. 4, no. 5, pp. 383–391, 2019.

[67] M. Lewerenz, A. Warnecke, and D. U. Sauer, "Post-mortem analysis on lifepo4| graphite cells describing the evolution & composition of covering layer on anode and their impact on cell performance," *Journal of Power Sources*, vol. 369, pp. 122–132, 2017.

[68] M. Lewerenz, A. Marongiu, A. Warnecke, and D. U. Sauer, "Differential voltage analysis as a tool for analyzing inhomogeneous aging: A case study for lifepo4| graphite cylindrical cells," *Journal of Power Sources*, vol. 368, pp. 57–67, 2017.

[69] X. Ma, J. E. Harlow, J. Li, *et al.*, "Hindering rollover failure of li [ni0. 5mn0. 3co0. 2] o2/graphite pouch cells during long-term cycling," *Journal of The Electrochemical Society*, vol. 166, no. 4, A711–A724, 2019.

[70] Y. Preger, H. M. Barkholtz, A. Fresquez, *et al.*, "Degradation of commercial lithium-ion cells as a function of chemistry and cycling conditions," *Journal of The Electrochemical Society*, vol. 167, no. 12, pp. 120–532, 2020.

[71] M. Lewerenz, J. Münnix, J. Schmalstieg, S. Käbitz, M. Knips, and D. U. Sauer, "Systematic aging of commercial lifepo4| graphite cylindrical cells including a theory explaining rise of capacity during aging," *Journal of Power Sources*, vol. 345, pp. 254–263, 2017.

[72] A. Pfrang, A. Kersys, A. Kriston, *et al.*, "Long-term cycling induced jelly roll deformation in commercial 18650 cells," *Journal of Power Sources*, vol. 392, pp. 168–175, 2018.

[73] A. Pfrang, A. Kersys, A. Kriston, *et al.*, "Geometrical inhomogeneities as cause of mechanical failure in commercial 18650 lithium ion cells," *Journal of The Electrochemical Society*, vol. 166, no. 15, A3745, 2019.

[74] M. Wünsch, J. Kaufman, and D. U. Sauer, "Investigation of the influence of different bracing of automotive pouch cells on cyclic lifetime and impedance spectra," *Journal of Energy Storage*, vol. 21, pp. 149–155, 2019.

[75] L. K. Willenberg, P. Dechent, G. Fuchs, D. U. Sauer, and E. Figgemeier, "High-precision monitoring of volume change of commercial lithium-ion batteries by using strain gauges," *Sustainability*, vol. 12, no. 2, p. 557, 2020.

[76] H. Zhang, F. Altaf, and T. Wik, "Scenario-aware machine learning pipeline for battery lifetime prediction," in *2024 European Control Conference (ECC)*, IEEE, 2024, pp. 212–217.

[77] M. Hassini, E. Redondo-Iglesias, and P. Venet, "Lithium–ion battery data: From production to prediction," *Batteries*, vol. 9, no. 7, p. 385, 2023.

[78] Q. Mayemba, R. Mingant, A. Li, G. Ducret, and P. Venet, "Aging datasets of commercial lithium-ion batteries: A review," *Journal of Energy Storage*, vol. 83, p. 110 560, 2024.

[79] G. Pozzato, A. Allam, and S. Onori, "Lithium-ion battery aging dataset based on electric vehicle real-driving profiles," *Data in Brief*, vol. 41, p. 107 995, 2022.

[80] N. Kirkaldy, M. A. Samieian, G. J. Offer, M. Marinescu, and Y. Patel, "Lithium-ion battery degradation: Comprehensive cycle ageing data and analysis for commercial 21700 cells," *Journal of Power Sources*, vol. 603, p. 234 185, 2024.

[81] H. Zhang, F. Altaf, and T. Wik, "Synthetic dataset of lg m50 batteries with different degradation pathways," *Data in Brief*, vol. 57, p. 111 076, 2024.

[82] H. Zhang, F. Altaf, and T. Wik, "Battery capacity knee-onset identification and early prediction using degradation curvature," *Journal of Power Sources*, vol. 608, p. 234 619, 2024.

[83] M. Doyle, T. F. Fuller, and J. Newman, "Modeling of galvanostatic charge and discharge of the lithium/polymer/insertion cell," *Journal of the Electrochemical society*, vol. 140, no. 6, p. 1526, 1993.

[84] S. G. Marquis, V. Sulzer, R. Timms, C. P. Please, and S. J. Chapman, "An asymptotic derivation of a single particle model with electrolyte," *Journal of The Electrochemical Society*, vol. 166, no. 15, A3693, 2019.

[85] F. Single, A. Latz, and B. Horstmann, "Identifying the mechanism of continued growth of the solid–electrolyte interphase," *ChemSusChem*, vol. 11, no. 12, pp. 1950–1955, 2018.

[86] B. Horstmann, F. Single, and A. Latz, "Review on multi-scale models of solid-electrolyte interphase formation," *Current Opinion in Electrochemistry*, vol. 13, pp. 61–69, 2019.

[87] P. Arora, M. Doyle, and R. E. White, "Mathematical modeling of the lithium deposition overcharge reaction in lithium-ion batteries using carbon-based negative electrodes," *Journal of The Electrochemical Society*, vol. 146, no. 10, p. 3543, 1999.

[88] H. Ge, T. Aoki, N. Ikeda, *et al.*, "Investigating lithium plating in lithium-ion batteries at low temperatures using electrochemical model with nmr assisted parameterization," *Journal of The Electrochemical Society*, vol. 164, no. 6, A1050, 2017.

[89] R. Deshpande, M. Verbrugge, Y.-T. Cheng, J. Wang, and P. Liu, "Battery cycle life prediction with coupled chemical degradation and fatigue mechanics," *Journal of the Electrochemical Society*, vol. 159, no. 10, A1730, 2012.

[90] I. Laresgoiti, S. Käbitz, M. Ecker, and D. U. Sauer, "Modeling mechanical degradation in lithium ion batteries during cycling: Solid electrolyte interphase fracture," *Journal of Power Sources*, vol. 300, pp. 112–122, 2015.

[91] F. M. Kindermann, J. Keil, A. Frank, and A. Jossen, "A sei modeling approach distinguishing between capacity and power fade," *Journal of The Electrochemical Society*, vol. 164, no. 12, E287, 2017.

[92] M. V. Micea, L. Ungurean, G. N. Cârstoiu, and V. Groza, "Online state-of-health assessment for battery management systems," *IEEE Transactions on Instrumentation and Measurement*, vol. 60, no. 6, pp. 1997–2006, 2011.

[93] C. Hu, H. Ye, G. Jain, and C. Schmidt, "Remaining useful life assessment of lithium-ion batteries in implantable medical devices," *Journal of Power Sources*, vol. 375, pp. 118–130, 2018.

[94] I. Bloom, B. Cole, J. Sohn, *et al.*, "An accelerated calendar and cycle life study of li-ion cells," *Journal of power sources*, vol. 101, no. 2, pp. 238–247, 2001.

[95] M. Broussely, S. Herreyre, P. Biensan, P. Kasztejna, K. Nechev, and R. Staniewicz, "Aging mechanism in li ion cells and calendar life predictions," *Journal of Power Sources*, vol. 97, pp. 13–21, 2001.

[96] J. Schmalstieg, S. Käbitz, M. Ecker, and D. U. Sauer, "A holistic aging model for $Li(NiMnCo)O_2$ based 18650 lithium-ion batteries," *Journal of Power Sources*, vol. 257, pp. 325–334, 2014.

[97] M. Schimpe, M. E. von Kuepach, M. Naumann, H. C. Hesse, K. Smith, and A. Jossen, "Comprehensive modeling of temperature-dependent degradation mechanisms in lithium iron phosphate batteries," *Journal of The Electrochemical Society*, vol. 165, no. 2, A181, 2018.

[98] B. Xu, A. Oudalov, A. Ulbig, G. Andersson, and D. S. Kirschen, "Modeling of lithium-ion battery degradation for cell life assessment," *IEEE Transactions on Smart Grid*, vol. 9, no. 2, pp. 1131–1140, 2016.

[99] J. Wang, P. Liu, J. Hicks-Garner, *et al.*, "Cycle-life model for graphite-lifepo4 cells," *Journal of power sources*, vol. 196, no. 8, pp. 3942–3948, 2011.

[100] B. Y. Liaw, G. Nagasubramanian, R. G. Jungst, and D. H. Doughty, "Modeling of lithium ion cells—a simple equivalent-circuit model approach," *Solid state ionics*, vol. 175, no. 1-4, pp. 835–839, 2004.

[101] B. Long, W. Xian, L. Jiang, and Z. Liu, "An improved autoregressive model by particle swarm optimization for prognostics of lithium-ion batteries," *Microelectronics Reliability*, vol. 53, no. 6, pp. 821–831, 2013.

[102] Y. Zhou and M. Huang, "Lithium-ion batteries remaining useful life prediction based on a mixture of empirical mode decomposition and arima model," *Microelectronics Reliability*, vol. 65, pp. 265–273, 2016.

[103] A. Nuhic, T. Terzimehic, T. Soczka-Guth, M. Buchholz, and K. Dietmayer, "Health diagnosis and remaining useful life prognostics of lithium-ion batteries using data-driven methods," *Journal of power sources*, vol. 239, pp. 680–688, 2013.

[104] T. Qin, S. Zeng, and J. Guo, "Robust prognostics for state of health estimation of lithium-ion batteries based on an improved PSO–SVR model," *Microelectronics Reliability*, vol. 55, no. 9-10, pp. 1280–1284, 2015.

[105] S. Voronov, E. Frisk, and M. Krysander, "Data-driven battery lifetime prediction and confidence estimation for heavy-duty trucks," *IEEE Transactions on Reliability*, vol. 67, no. 2, pp. 623–639, 2018.

[106] F. Yang, D. Wang, F. Xu, Z. Huang, and K.-L. Tsui, "Lifespan prediction of lithium-ion batteries based on various extracted features and gradient boosting regression tree model," *Journal of Power Sources*, vol. 476, p. 228 654, 2020.

[107] Y. Zhang, R. Xiong, H. He, and M. G. Pecht, "Long short-term memory recurrent neural network for remaining useful life prediction of lithium-ion batteries," *IEEE Transactions on Vehicular Technology*, vol. 67, no. 7, pp. 5695–5705, 2018.

[108] L. Ren, J. Dong, X. Wang, Z. Meng, L. Zhao, and M. J. Deen, "A data-driven auto-cnn-lstm prediction model for lithium-ion battery remaining useful life," *IEEE Transactions on Industrial Informatics*, vol. 17, no. 5, pp. 3478–3487, 2020.

[109] K. Liu, Q. Peng, H. Sun, M. Fei, H. Ma, and T. Hu, "A transferred recurrent neural network for battery calendar health prognostics of energy-transportation systems," *IEEE Transactions on Industrial Informatics*, vol. 18, no. 11, pp. 8172–8181, 2022.

[110] R. R. Richardson, M. A. Osborne, and D. A. Howey, "Battery health prediction under generalized conditions using a gaussian process transition model," *Journal of Energy Storage*, vol. 23, pp. 320–328, 2019.

[111] H. Li, D. Pan, and C. P. Chen, "Intelligent prognostics for battery health monitoring using the mean entropy and relevance vector machine," *IEEE Transactions on Systems, Man, and Cybernetics: Systems*, vol. 44, no. 7, pp. 851–862, 2014.

[112] D. Liu, J. Zhou, D. Pan, Y. Peng, and X. Peng, "Lithium-ion battery remaining useful life estimation with an optimized relevance vector machine algorithm with incremental learning," *Measurement*, vol. 63, pp. 143–151, 2015.

[113] H. Zhang, Y. Su, F. Altaf, T. Wik, and S. Gros, "Interpretable battery cycle life range prediction using early cell degradation data," *IEEE Transactions on Transportation Electrification*, 2022.

[114] S. Zhang, Z. Liu, and H. Su, "A bayesian mixture neural network for remaining useful life prediction of lithium-ion batteries," *IEEE Transactions on Transportation Electrification*, vol. 8, no. 4, pp. 4708–4721, 2022.

[115] M. Aykol, C. B. Gopal, A. Anapolsky, *et al.*, "Perspective—combining physics and machine learning to predict battery lifetime," *Journal of The Electrochemical Society*, vol. 168, no. 3, p. 030 525, 2021.

[116] G. E. Karniadakis, I. G. Kevrekidis, L. Lu, P. Perdikaris, S. Wang, and L. Yang, "Physics-informed machine learning," *Nature Reviews Physics*, vol. 3, no. 6, pp. 422–440, 2021.

[117] M.-F. Ng, J. Zhao, Q. Yan, G. J. Conduit, and Z. W. Seh, "Predicting the state of charge and health of batteries using data-driven machine learning," *Nature Machine Intelligence*, vol. 2, no. 3, pp. 161–170, 2020.

[118] S. Atlung, K. West, and T. Jacobsen, "Dynamic aspects of solid solution cathodes for electrochemical power sources," *Journal of The Electrochemical Society*, vol. 126, no. 8, p. 1311, 1979.

[119] G. Ning and B. N. Popov, "Cycle life modeling of lithium-ion batteries," *Journal of The Electrochemical Society*, vol. 151, no. 10, A1584, 2004.

[120] P. Ramadass, B. Haran, P. M. Gomadam, R. White, and B. N. Popov, "Development of first principles capacity fade model for li-ion cells," *Journal of the Electrochemical Society*, vol. 151, no. 2, A196, 2004.

[121] N. A. Chaturvedi, R. Klein, J. Christensen, J. Ahmed, and A. Kojic, "Algorithms for advanced battery-management systems," *IEEE Control systems magazine*, vol. 30, no. 3, pp. 49–68, 2010.

[122] S. Santhanagopalan, Q. Guo, and R. E. White, "Parameter estimation and model discrimination for a lithium-ion cell," *Journal of the Electrochemical Society*, vol. 154, no. 3, A198, 2007.

[123] V. A. Agubra and J. W. Fergus, "The formation and stability of the solid electrolyte interface on the graphite anode," *Journal of Power Sources*, vol. 268, pp. 153–162, 2014.

[124] H. J. Ploehn, P. Ramadass, and R. E. White, "Solvent diffusion model for aging of lithium-ion battery cells," *Journal of The Electrochemical Society*, vol. 151, no. 3, A456, 2004.

[125] M. Tang, S. Lu, and J. Newman, "Experimental and theoretical investigation of solid-electrolyte-interphase formation mechanisms on glassy carbon," *Journal of The Electrochemical Society*, vol. 159, no. 11, A1775, 2012.

[126] L. Liu, J. Park, X. Lin, A. M. Sastry, and W. Lu, "A thermal-electrochemical model that gives spatial-dependent growth of solid electrolyte interphase in a li-ion battery," *Journal of power sources*, vol. 268, pp. 482–490, 2014.

[127] X.-G. Yang, S. Ge, T. Liu, Y. Leng, and C.-Y. Wang, "A look into the voltage plateau signal for detection and quantification of lithium plating in lithium-ion cells," *Journal of Power Sources*, vol. 395, pp. 251–261, 2018.

[128] C. von Lüders, J. Keil, M. Webersberger, and A. Jossen, "Modeling of lithium plating and lithium stripping in lithium-ion batteries," *Journal of Power Sources*, vol. 414, pp. 41–47, 2019.

[129] S. E. O'Kane, I. D. Campbell, M. W. Marzook, G. J. Offer, and M. Marinescu, "Physical origin of the differential voltage minimum associated with lithium plating in li-ion batteries," *Journal of The Electrochemical Society*, vol. 167, no. 9, p. 090 540, 2020.

[130] J. Li, K. Adewuyi, N. Lotfi, R. G. Landers, and J. Park, "A single particle model with chemical/mechanical degradation physics for lithium ion battery state of health (soh) estimation," *Applied energy*, vol. 212, pp. 1178–1190, 2018.

[131] L. Lu, P. Jin, G. Pang, Z. Zhang, and G. E. Karniadakis, "Learning nonlinear operators via deeponet based on the universal approximation theorem of operators," *Nature machine intelligence*, vol. 3, no. 3, pp. 218–229, 2021.

[132] Z. Li, N. Kovachki, K. Azizzadenesheli, *et al.*, "Fourier neural operator for parametric partial differential equations," *arXiv preprint arXiv:2010.08895*, 2020.

[133] Y. LeCun, Y. Bengio, *et al.*, "Convolutional networks for images, speech, and time series," *The handbook of brain theory and neural networks*, vol. 3361, no. 10, p. 1995, 1995.

[134] M. M. Bronstein, J. Bruna, Y. LeCun, A. Szlam, and P. Vandergheynst, "Geometric deep learning: Going beyond euclidean data," *IEEE Signal Processing Magazine*, vol. 34, no. 4, pp. 18–42, 2017.

[135] M. Raissi, P. Perdikaris, and G. E. Karniadakis, "Numerical gaussian processes for time-dependent and nonlinear partial differential equations," *SIAM Journal on Scientific Computing*, vol. 40, no. 1, A172–A198, 2018.

[136] J. Sirignano and K. Spiliopoulos, "Dgm: A deep learning algorithm for solving partial differential equations," *Journal of computational physics*, vol. 375, pp. 1339–1364, 2018.

[137] M. Raissi, P. Perdikaris, and G. E. Karniadakis, "Physics-informed neural networks: A deep learning framework for solving forward and inverse problems involving nonlinear partial differential equations," *Journal of Computational physics*, vol. 378, pp. 686–707, 2019.

[138] Y. Huang, C. Zou, Y. Li, and T. Wik, "Minn: Learning the dynamics of differential-algebraic equations and application to battery modeling," *IEEE Transactions on Pattern Analysis and Machine Intelligence*, 2024.

[139] V. Sulzer, P. Mohtat, A. Aitio, *et al.*, "The challenge and opportunity of battery lifetime prediction from field data," *Joule*, vol. 5, no. 8, pp. 1934–1955, 2021.

[140] E. Braco, I. San Martin, P. Sanchis, A. Ursúa, and D.-I. Stroe, "Health indicator selection for state of health estimation of second-life lithium-ion batteries under extended ageing," *Journal of Energy Storage*, vol. 55, p. 105 366, 2022.

[141] M. Arrinda, M. Oyarbide, H. Macicior, *et al.*, "Application dependent end-of-life threshold definition methodology for batteries in electric vehicles," *Batteries*, vol. 7, no. 1, p. 12, 2021.

[142] J. Keil and A. Jossen, "Electrochemical modeling of linear and nonlinear aging of lithium-ion cells," *Journal of The Electrochemical Society*, vol. 167, no. 11, p. 110 535, 2020.

[143] H. Ekström and G. Lindbergh, "A model for predicting capacity fade due to sei formation in a commercial graphite/lifepo4 cell," *Journal of The Electrochemical Society*, vol. 162, no. 6, A1003, 2015.

[144] S. Atalay, M. Sheikh, A. Mariani, Y. Merla, E. Bower, and W. D. Widanage, "Theory of battery ageing in a lithium-ion battery: Capacity fade, nonlinear ageing and lifetime prediction," *Journal of Power Sources*, vol. 478, p. 229 026, 2020.

[145] F. Yang, X. Song, G. Dong, and K.-L. Tsui, "A coulombic efficiency-based model for prognostics and health estimation of lithium-ion batteries," *Energy*, vol. 171, pp. 1173–1182, 2019.

[146] Z. Fei, F. Yang, K.-L. Tsui, L. Li, and Z. Zhang, "Early prediction of battery lifetime via a machine learning based framework," *Energy*, vol. 225, p. 120 205, 2021.

[147] N. H. Paulson, J. Kubal, L. Ward, S. Saxena, W. Lu, and S. J. Babinec, "Feature engineering for machine learning enabled early prediction of battery lifetime," *Journal of Power Sources*, vol. 527, p. 231 127, 2022.

[148] S. Greenbank and D. Howey, "Automated feature extraction and selection for data-driven models of rapid battery capacity fade and end of life," *IEEE Transactions on Industrial Informatics*, vol. 18, no. 5, pp. 2965–2973, 2021.

[149] M. Etxandi-Santolaya, L. C. Casals, and C. Corchero, "Extending the electric vehicle battery first life: Performance beyond the current end of life threshold," *Heliyon*, vol. 10, no. 4, 2024.

[150] G. B. Alliance *et al.*, "A vision for a sustainable battery value chain in 2030: Unlocking the full potential to power sustainable development and climate change mitigation," in *Geneva, Switzerland: World Economic Forum*, 2019, pp. 1–52.

[151] W. Gao, Z. Cao, Y. Fu, *et al.*, "Comprehensive study of the aging knee and second-life potential of the nissan leaf e+ batteries," *Journal of Power Sources*, vol. 613, p. 234 884, 2024.

[152] IEEE Power and Energy Society, "IEEE Recommended Practice for Sizing Lead-Acid Batteries for Stationary Applications," *IEEE Std 485-2020 (Revision of IEEE Std 485-2010)*, pp. 1–69, 2020.

[153] W. Diao, S. Saxena, B. Han, and M. Pecht, "Algorithm to determine the knee point on capacity fade curves of lithium-ion cells," *Energies*, vol. 12, no. 15, p. 2910, 2019.

[154] P. Fermín-Cueto, E. McTurk, M. Allerhand, *et al.*, "Identification and machine learning prediction of knee-point and knee-onset in capacity degradation curves of lithium-ion cells," *Energy and AI*, vol. 1, p. 100 006, 2020.

[155] C. Zhang, Y. Wang, Y. Gao, F. Wang, B. Mu, and W. Zhang, "Accelerated fading recognition for lithium-ion batteries with nickel-cobalt-manganese cathode using quantile regression method," *Applied Energy*, vol. 256, p. 113 841, 2019.

[156] S. Sohn, H.-E. Byun, and J. H. Lee, "Two-stage deep learning for online prediction of knee-point in li-ion battery capacity degradation," *Applied Energy*, vol. 328, p. 120 204, 2022.

[157] N. Costa, D. Anseán, M. Dubarry, and L. Sánchez, "Icformer: A deep learning model for informed lithium-ion battery diagnosis and early knee detection," *Journal of Power Sources*, vol. 592, p. 233 910, 2024.

[158] D. W. Bacon and D. G. Watts, "Estimating the transition between two intersecting straight lines," *Biometrika*, vol. 58, no. 3, pp. 525–534, 1971.

[159] R. Xiong, Y. Pan, W. Shen, H. Li, and F. Sun, "Lithium-ion battery aging mechanisms and diagnosis method for automotive applications: Recent advances and perspectives," *Renewable and Sustainable Energy Reviews*, vol. 131, p. 110 048, 2020.

[160] T. Waldmann, M. Wilka, M. Kasper, M. Fleischhammer, and M. Wohlfahrt-Mehrens, "Temperature dependent ageing mechanisms in lithium-ion batteries–a post-mortem study," *Journal of power sources*, vol. 262, pp. 129–135, 2014.

[161] T. Waldmann, A. Iturrondobeitia, M. Kasper, *et al.*, "Post-mortem analysis of aged lithium-ion batteries: Disassembly methodology and physico-chemical analysis techniques," *Journal of The Electrochemical Society*, vol. 163, no. 10, A2149, 2016.

[162] T. Waldmann, J. B. Quinn, K. Richter, *et al.*, "Electrochemical, post-mortem, and arc analysis of li-ion cell safety in second-life applications," *Journal of The Electrochemical Society*, vol. 164, no. 13, A3154, 2017.

[163] T. Waldmann, N. Ghanbari, M. Kasper, and M. Wohlfahrt-Mehrens, "Correlations between electrochemical data and results from post-mortem analysis of aged lithium-ion batteries," *Journal of the Electrochemical Society*, vol. 162, no. 8, A1500, 2015.

[164] U. Golla-Schindler, D. Zeibig, L. Prickler, S. Behn, T. Bernthaler, and G. Schneider, "Characterization of degeneration phenomena in lithium-ion batteries by combined microscopic techniques," *Micron*, vol. 113, pp. 10–19, 2018.

[165] M. S. D. Darma, M. Lang, K. Kleiner, *et al.*, "The influence of cycling temperature and cycling rate on the phase specific degradation of a positive electrode in lithium ion batteries: A post mortem analysis," *Journal of Power Sources*, vol. 327, pp. 714–725, 2016.

[166] T. Schwieters, M. Evertz, M. Mense, M. Winter, and S. Nowak, "Lithium loss in the solid electrolyte interphase: Lithium quantification of aged lithium ion battery graphite electrodes by means of laser ablation inductively coupled plasma mass spectrometry and inductively coupled plasma optical emission spectroscopy," *Journal of power sources*, vol. 356, pp. 47–55, 2017.

[167] N. Kimura, E. Seki, H. Konishi, *et al.*, "Cycle deterioration analysis of 0.6 ah-class lithium-ion cells with cell chemistry of lini0. 6co0. 2mn0. 2o2-based/graphite," *Journal of Power Sources*, vol. 332, pp. 187–192, 2016.

[168] R. Xiong, L. Li, Z. Li, Q. Yu, and H. Mu, "An electrochemical model based degradation state identification method of lithium-ion battery for all-climate electric vehicles application," *Applied energy*, vol. 219, pp. 264–275, 2018.

[169] J. Kim, H. Chun, M. Kim, S. Han, J.-W. Lee, and T.-K. Lee, "Effective and practical parameters of electrochemical li-ion battery models for degradation diagnosis," *Journal of Energy Storage*, vol. 42, p. 103 077, 2021.

[170] G. Fan, D. Lu, M. S. Trimboli, G. L. Plett, C. Zhu, and X. Zhang, "Nondestructive diagnostics and quantification of battery aging under different degradation paths," *Journal of Power Sources*, vol. 557, p. 232 555, 2023.

[171] R. Fu, S.-Y. Choe, V. Agubra, and J. Fergus, "Modeling of degradation effects considering side reactions for a pouch type li-ion polymer battery with carbon anode," *Journal of Power Sources*, vol. 261, pp. 120–135, 2014.

[172] M. Safari, M. Morcrette, A. Teyssot, and C. Delacourt, "Multimodal physics-based aging model for life prediction of li-ion batteries," *Journal of The Electrochemical Society*, vol. 156, no. 3, A145, 2008.

[173] S. J. Harris and P. Lu, "Effects of inhomogeneities–nanoscale to mesoscale–on the durability of li-ion batteries," *The Journal of Physical Chemistry C*, vol. 117, no. 13, pp. 6481–6492, 2013.

[174] J. Zhu, T. Wierzbicki, and W. Li, "A review of safety-focused mechanical modeling of commercial lithium-ion batteries," *Journal of Power Sources*, vol. 378, pp. 153–168, 2018.

[175] M. K. Al-Alawi, J. Cugley, and H. Hassanin, "Techno-economic feasibility of retired electric-vehicle batteries repurpose/reuse in second-life applications: A systematic review," *Energy and Climate Change*, p. 100 086, 2022.

[176] B. Zou, J. Peng, S. Li, Y. Li, J. Yan, and H. Yang, "Comparative study of the dynamic programming-based and rule-based operation strategies for grid-connected pv-battery systems of office buildings," *Applied energy*, vol. 305, p. 117 875, 2022.

[177] J. B. Rawlings, D. Q. Mayne, M. Diehl, *et al.*, *Model predictive control: theory, computation, and design*. Nob Hill Publishing Madison, WI, 2017, vol. 2.

[178] J. Hu, Y. Shan, J. M. Guerrero, A. Ioinovici, K. W. Chan, and J. Rodriguez, "Model predictive control of microgrids–an overview," *Renewable and Sustainable Energy Reviews*, vol. 136, p. 110 422, 2021.

[179] R. S. Sutton, A. G. Barto, *et al.*, *Reinforcement learning: An introduction*. MIT press Cambridge, 1998, vol. 1.

[180] W. Cai, A. B. Kordabad, and S. Gros, "Energy management in residential microgrid using model predictive control-based reinforcement learning and shapley value," *Engineering Applications of Artificial Intelligence*, vol. 119, p. 105 793, 2023.